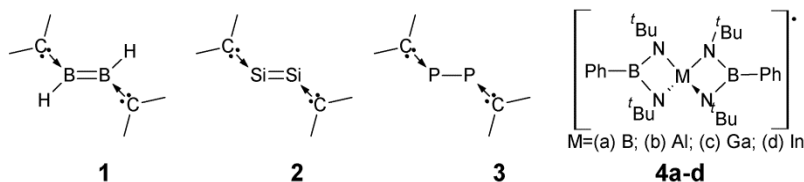


Inorganic and Organometallic Radicals of Main Group Elements (2010-2011)René T. Boéré^a^a Department of Chemistry and Biochemistry, University of Lethbridge, Lethbridge, AB, Canada T1K3M4**1 Introduction**

The primary literature and a sampling of key review articles published during 2010 - 2011 are covered along with some additional papers drawn from 2009 where necessary to provide continuity and from the beginning of 2012. The review period has been very fertile for the development of open-shell main group element compounds and materials. While coverage is not exhaustive, the intent has been to indicate those areas that have seen the greatest activity. As well, isolated reports considered significant have been included, which may signal profitable areas for further investigation. Some overlap with the huge field of organic materials is inevitable in any such treatment, yet all but the most relevant carbon-containing radicals are excluded, as are *d* and *f*-element paramagnets. Readers may detect a bias in favour of systems that are electrochemically characterised, especially where EPR spectroelectrochemistry was employed. Finally, no coverage is provided for the burgeoning field of “biradicaloids” as these rarely have interesting electrochemical or EPR spectroscopic properties. A significant event during the review period was publication of the book-length treatment *Stable Radicals: Fundamentals and Applied Aspects of Odd-Electron Compounds*, written by a series of experts and edited by Robin Hicks.¹ Particular strengths of this work are the inclusion of both main group *and* organic radicals fairly even-handedly and also a strong focus on applications including polymerization, molecular magnetism, battery technology and EPR imaging. Unfortunately, only neutral radicals are covered whereas cation and anion radicals feature prominently amongst main group element species.

Four recent reviews serve to emphasize the tremendous impact that “N-heterocyclic carbenes” (NHC) with very bulky substituents on the two nitrogen atoms are having on main group element chemistry.^{2,3,4,5} These powerful new Lewis bases serve to stabilize “naked” elements as well as multiply bonded diatomics. The breakthrough discovery involved the stabilization of the diborene L:HB=BH:L **1**,⁶ this was followed by the isolation and structural characterization of a disilene complex L:Si=Si:L **2**⁷ and a similar carbene-stabilized L:P₂:L complex **3**.⁸ Although there are numerous ways to describe the electronic structures of these adducts, the net effect is that they are electron rich and thus readily oxidized to new open-shell species, several of which are mentioned below. The NHC approach is thus reminiscent of using “overcharged” ligands such as boramidinate²⁻ to create anionic complexes with, for example, group 13 elements, that can readily be oxidized to the stable neutral radicals **4**.^{9,10} Two recently discovered radical-based hysteretic materials have been singled out for their potential as molecular materials with switching/sensing applications.^{11,12,13} EPR spectroscopy could (but has not yet been) used as a sensor for such switching behaviour.



Abbreviations and conventions adopted: A, hyperfine coupling (hfc) constant (in MHz); a , hyperfine splitting (HFS) constant (in mT); CV, cyclic voltammetry; DFT, density functional theory; NHC, *N*-heterocyclic carbene; CAAC, cyclic alkyl-amino carbene; Dipp, 2,6-diisopropylphenyl; DMSO, dimethyl sulphoxide; DME, 1,2-dimethoxyethane; DMF, dimethylformamide; THF, tetrahydrofuran; hfac, hexafluoroacetylacetonate; LW, peak-to-trough EPR linewidths; Mes, 2,4,6-trimethylphenyl; $\text{Fc}^{0/+}$, refers to the ferrocene/ferrocenium redox couple, the IUPAC-recommended reference for non-aqueous solvent electrochemistry. Wherever possible, quoted electrochemistry data is presented on this scale with $E_{1/2}(\text{Fc}^{0/+}) = 0 \text{ V}$, if necessary using published conversions.^{14,15}

2 New and improved methods

Whilst the basic methodology of electrochemistry (voltammetry and electrolysis) as well as EPR spectroscopy is now quite mature, EPR spectroelectrochemistry remains a challenge and several methodological papers deserve mention. A very useful tutorial-review appeared that treats a variety of spectroelectrochemical methods including *in situ* EPR-electrochemistry.¹⁶ Although most of the examples discussed therein are either organic or transition metal coordination compounds, the principles are fully transferrable to main group chemistry. A paper by Moraes *et al.* uses the combined EPR/UVvis spectroelectrochemical cell originally developed by Neudeck and Kress in a study of the charging of poly(aniline boronic acid),¹⁷ nicely illustrating the power of combining both spectroscopies in conjunction with a UV-transmission EPR cavity.¹⁸ The Neudeck and Kress design has been miniaturized successfully for work in a low temperature flat cell.¹⁹

A newly developed *in situ* electrochemical cell for Q- and W-band EPR spectroscopy has been reported (Fig. 1i).²⁰ An obvious advantage over previous designs based on flat cells is the ability to rapidly cool samples containing electrogenerated radicals for observation in frozen solution. A more ambitious approach was taken in the design and use of a novel flow-through four-electrode EPR spectroelectrochemical cell specifically designed for two-stage electrogeneration of short-lived radicals (Fig. 1ii).²¹ In a primary compartment, preparative electrolysis is undertaken (for example a high-applied voltage reduction of an element-halide to an element anion); the second stage is typically under reverse bias and in close proximity to the sensitive region of the resonant cavity (for example, the oxidation of a long-lived element anion to a reactive free radical). This innovative and inexpensive flow-cell design seems to have a great potential for further investigations of reactive main group element radicals.

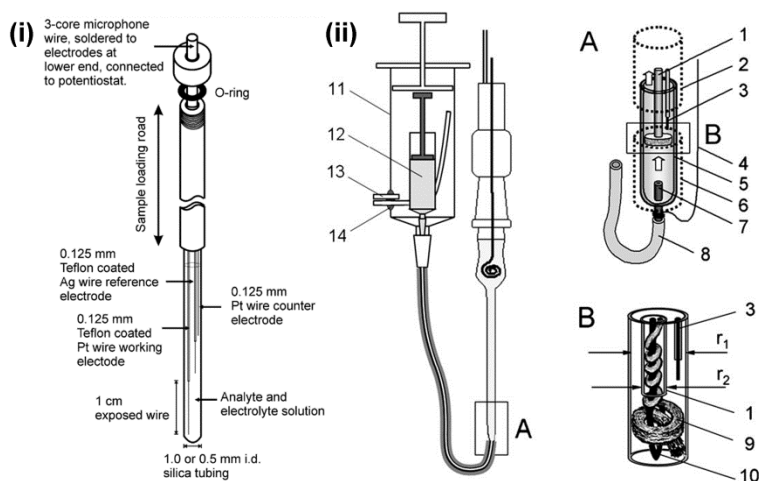


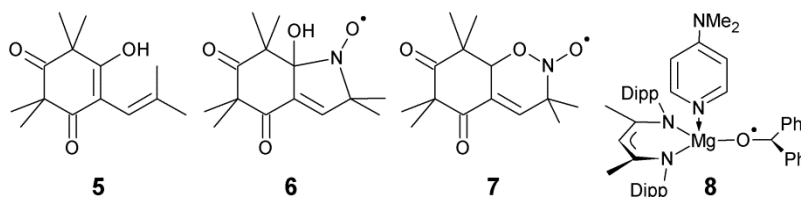
Figure 1. (i) Schematic diagram of Q/W-band EPR *in situ* spectroelectrochemical cell (lateral dimension not to scale for the sake of clarity). Reproduced with permission from ref. 20. (ii) Flow-through four-electrode electrochemical EPR cell and the solution supply syringe. A: The whole cell assembly and the electrode area enlargement, B: central part/working electrode enlargement. (1) Pyrex capillary isolating the Pt wire connector of the working electrode; (2) upper Al foil shield; (3) capillary sealed quasi-reference electrode; (4) contact wire for lower counter electrode; (5) Pyrex body of the EPR cell; (6) lower Al shield; (7) tubular Pt counter electrode; (8) PTFE solution inlet tube; (9) GC fiber working electrode; (10) Pt wire contact for working electrode; (11) casing syringe; (12) solution in the internal syringe; (13) argon inlet/outlet; (14) silicone sealing. Reproduced with permission from ref. 21.

3 Small open-shell inorganic molecules

3.1 Nitrogen oxide radicals

The nitrogen oxides remain the oldest and best-known main group element free radicals. A very thorough and up-to-date account of nitrogen oxide radicals is provided in the book chapter by Bohle.²² The modern organic chemistry of NO[•] has also been comprehensively reviewed.²³ It is well known that free NO[•] cannot be observed by EPR spectroscopy in condensed phases. However, when NO[•] is adsorbed to a surface, an EPR signal may be observed due to (i) quenching of the orbital angular momentum by the electric field of the adsorption site which transforms $^2\Pi_{1/2}$ into a pure spin state, and (ii) lifting of the degeneracy of the $2\pi^*$ orbitals with the result that the $2\pi_x^*/2\pi_y^*$ splitting energy controls the *g* value of the adsorbed NO[•] at close to the free-electron value (2.002). In fact, NO[•] is one of the most important probes for surfaces of metal oxides MO_x (M = Mg, Zn, Ti, Al, Sn, Ce) and the closely related zeolites as interpreted through (anisotropic) EPR spectra which display intense signals with large *g*- and *a*-value anisotropies.²⁴ These workers also monitored the effect of concentration which shows a decrease in signal intensity above 2×10^{19} molecules·g⁻¹ which is attributed to formation of the diamagnetic dimers (NO)₂. A detailed and informative review of the use of surface-localized inorganic radicals to probe surfaces has recently been published.²⁵

Detection of NO[•] in solution depends on the use of suitable spin traps (a spin trap is a species that interacts with a free-radical to produce a secondary radical favourable for EPR detection under the applicable environmental conditions). Here, coordination to a metal ion has a similar effect to that observed in surface probes as just mentioned. The most important assay for NO[•] in solution and in biological samples uses the dithiocarbamate complex [Fe(S₂CNEt₂)₂]; this complex, like NO[•],²⁶ on its own is EPR silent but the adduct [Fe(S₂CNEt₂)₂(NO)[•]] displays a characteristic triplet EPR signal with *g* = 2.035-2.040 and *a*(¹⁴N) = 1.26 mT.²⁶ However, alternatives to this common assay are valuable such as the organic chelotropic trap **5** suitable for spin-trapping of both NO[•], **6**, and NO₂[•], **7**.²⁷



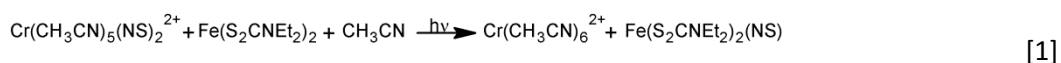
The transition-metal chemistry of the nitrosyl ligand has seen a tremendous revival since the discovery of nitric oxide as an essential biological molecule.²⁸ While there are many ways to synthesize nitrosyl complexes, the reaction of a metal nitride complex with an oxygen source is important because this method can be extended

to heavier chalcogens.²⁹ A similar reaction has been reported for an unusual square planar ruthenium complex $[(\text{N}(\text{SiMe}_2\text{CH}_2\text{P}^t\text{Bu}_2)_2)\text{RuN}]$.³⁰ The first insertion reactions of NO^\bullet into lanthanide-carbon bonds has recently been reported³¹ and $[\text{H}(\text{CH}_3)_4\text{C}_5]_3\text{UNO}$ is the first *f*-element nitrosyl complex.³² An EPR study of the nitroprusside trianion $[(\text{NC})_5\text{Fe}(\text{NO})]^{3-}$ provides support for NO^\bullet as a ligand in the radical state,³³ and linkage isomerism in the same complex has been studied by transient IR spectroscopy.³⁴ The non-innocence of NO^\bullet in nitrosyl ruthenium complexes has been stressed.³⁵

3.2 Nitrogen monosulfide, NS^\bullet and heavy congeners

There has been intense interest in the unstable radical NS^\bullet since it was detected by rotational spectroscopy in the coma of the comet Hale-Bopp and its rate of production was found to be at least a few hundredth of a per cent compared to water, with a total column density of $6.8 \times 10^{12} \text{ cm}^{-2}$.³⁶ The half-life of NS^\bullet was found to be between 5000 and 10^5 s with an expectation that it would be destroyed by solar photoionization. In order to clarify issues raised by the Halle-Bopp discovery, CCSD(T)/6-311++G(3df,3pd) calculations were used to study the formation of ^2NS from different reactions paths. The only energetically favourable and spin-allowed reaction path these workers could find is the reaction $^1\text{NH} + ^2\text{SH} \rightarrow ^2\text{NS} + \text{H}_2$ for which $\Delta H^\circ = -154 \text{ kJ}\cdot\text{mol}^{-1}$.³⁷ Metal thionitrosyl complexes remain of considerable interest. Just as for nitrosyl, there are two fundamental ways to make thionitrosyl complexes. The first uses one of several sources containing an NS unit (but never NS^\bullet itself unlike the case for NO^\bullet .) The second approach is both more elegant and versatile and involves building the N-E unit at the metal centre from a pre-existing metal nitride. Recent examples include osmium nitrides Li_2S ,³⁸ or sodium thiosulfate.³⁹ Similar approaches have been shown to work for rhenium.^{40,41} Typical $\nu(\text{NS})$ stretching frequencies range from ca. 1065 cm^{-1} for low-valent to 1390 cm^{-1} for high-valent metal complexes,⁴² values which clearly bracket the 1204 cm^{-1} value for this band in the gas-phase radical.

In an important series of papers, the novel $S = \frac{1}{2}$ thionitrosyl complexes $[\text{Cr}(\text{NS})(\text{CN})_5]^{3-}$, $[\text{Cr}(\text{NS})(\text{DMSO})_5]^{2+}$, $[\text{Cr}(\text{NS})(N\text{-methylformamide})_5]^{2+}$ and $[\text{Cr}(\text{NS})(\text{H}_2\text{O})_5]^{2+}$ have been prepared and investigated by EPR spectroscopy and their electronic structures compared to related NO and NSe complexes.^{26,43,44} Most significantly, the related $[\text{Cr}(\text{NS})(\text{NCCH}_3)_5]^{2+}$ has been shown to release NS^\bullet upon flash or continuous photolysis, and the NS^\bullet could be trapped by the classical nitric oxide spin trap $[\text{Fe}(\text{S}_2\text{CNET}_2)_2]$ (Equation 1).⁴⁴ This represents the first example of well-characterized chemical reactivity of NS^\bullet in solution. Moreover, it shows that the iron dithiocarbamate complex can function as a suitable spin trap for nitrogen monosulfide exactly as it does for NO^\bullet . By careful comparison of the behaviour of the nitrogen monoxide and nitrogen monosulfide systems, this study found evidence for partial consumption of NS^\bullet during the chromium to iron transfer reaction, which was attributed to NS^\bullet oligomerisation processes.⁴⁴



Interest in NSe^\bullet and NTe^\bullet is less driven by astrophysics than is the case for NS^\bullet ; however one recent report includes NTe^\bullet in a study estimating the Kronecker product periodic system of diatomics by statistical methods for the purpose of establishing radiative transfer models for earth and interstellar atmospheres.⁴⁵

3.3 Oxygen radicals

The first direct *in situ* EPR spectroelectrochemical evidence for the superoxide anion radical has been reported.⁴⁶ While the electrochemical production of $\text{OO}^{\bullet-}$ is quite common, small amounts of water will lead to

protonation of superoxide and subsequently to a formation of hydrogen peroxide. Therefore, a direct proof using the magnetic property of $\text{OO}^{\bullet-}$ is very desirable. Free $\text{OO}^{\bullet-}$ has a 2-fold orbital degeneracy in the electronic ground state, which frustrates observation of the EPR signal as mentioned above for NO^{\bullet} . This degeneracy can be lifted by even a weak coordinate bond; in this report, $\text{OO}^{\bullet-}$ was detected in DMSO at 280 K by generating it in the presence of potassium-crown-ether as the counter ion, resulting in an intense singlet with very little g anisotropy in the EPR spectrum.

A gas-phase EPR study shows that OONO^{\bullet} ($g = 2.014$) is an intermediate ($t_{1/2} = 0.1$ s) in the autoxidation of NO^{\bullet} .⁴⁷ These workers also isolated a red substance ($\lambda_{\text{max}} = 500$ nm) from the reaction at high concentration of nitric oxide and oxygen in 2-methylbutane at 113 K which they assign to ONOONO , i.e. from further reaction of the peroxyxynitrite radical with a second equivalent of NO^{\bullet} . The EPR spectrum of OONO^{\bullet} was previously detected in a frozen H_2SO_4 matrix and is axial with $g_{11} = 2.048$, $g_{22,33} = 2.003$ and $a(^{14}\text{N}) = 0.35$ mT.⁴⁸ A recent matrix study employing the co-deposition of $\text{Ne}/\text{NO}^{\bullet}$ and Ne/O_2 discovered strong, structured charge-transfer bands with a $\lambda_{\text{max}} = 275$ nm attributed to transfer of an electron from NO^{\bullet} to O_2 in a weak van der Waals complex between the two.⁴⁹ A very thorough matrix infra-red study supports the two-step mechanism for the auto-oxidation of NO^{\bullet} first proposed by McKee.^{50,51} Two detailed computational studies at the CAS level of theory have investigated this mechanism. These workers found that a balanced treatment of both dynamic and static electron correlation is necessary for the correct energy estimation for intermediates; when this is taken into account it provides strong support for the two-step mechanism of NO^{\bullet} oxidation.^{52,53}

A related species that is of intense current interest to the biological role of NO^{\bullet} is the peroxyxynitrite ion OONO^- which is formed by the fast spin-allowed reaction between nitric oxide and superoxide anion radical: $\text{NO}^{\bullet} + \text{OO}^{\bullet-} \rightarrow \text{OONO}^-$. A fascinating voltammetric experiment using microelectrodes in a human tissue cell (fibroblast) has resulted in measurement of the electrical signature for the oxidation of peroxyxynitrite with $E^0 = +0.27$ vs. SCE; the lifetime of the electrogenerated OONO^{\bullet} radical was determined as $t_{1/2} \approx 0.1$ s.⁵⁴ This discovery has become the basis of several assays for the detection of OONO^- .⁵⁵

The reactivity of small oxygen-centred radicals has also been highlighted in two further examples.⁵⁶ A combined mass spectrometric/computational study showed that the $\text{SO}_2^{\bullet+}$ radical cation efficiently activates methane at room temperature through a $[\text{H}_3\text{C}^{\bullet}\cdots\text{HOSO}^+]$ methyl intermediate isolated in the gas phase by mass spectrometry.⁵⁷ Methanol and ionized methyl hydrogen sulphoxylate, $\text{CH}_3\text{OSOH}^{\bullet+}$, are formed by selective, direct attack of the incipient methyl radical at the O atom of the intermediate. A combination of mass spectrometry and computational studies shows that the polynuclear non-metal oxide cation $[\text{P}_4\text{O}_{10}]^+$ is also capable of activating the C–H bond of methane at room temperature.⁵⁸

4 Group 2 elements

The novel magnesium ketyl radical **8**, formed by reduction of benzophenone with a dimeric Mg(I) complex in the presence of dimethylaminopyridine, has been reported.⁵⁹ Using CW EPR, ENDOR and special TRIPLE resonance, the spin distribution in the radical has been explored at variable temperatures (200–298 K). At 298 K, most of the unpaired spin is found to be confined to the $(\text{OCPh}_2^{\bullet})$ fragment based on the hfc: $A(^1\text{H}_{\text{ortho}}) = 8.30$, $A(^1\text{H}_{\text{meta}}) = 3.00$ and $A(^1\text{H}_{\text{para}}) = 9.95$ MHz.

5 Boron

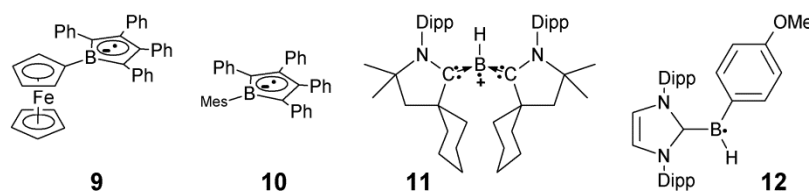
Recent chemistry involving open-shell boron compounds, previously thought to be poor candidates for free radicals, has been reviewed in two publications.^{60,61} Several points discussed below are mentioned in these works: (i) examples of boron radical anions isoelectronic with organonitrogen radical cations; (ii) aminoborane radical anions and (iii) incorporation of boron into planar aromatic molecules. However, the largest numbers of boron radicals remain polyborane cluster radical anions, $[B_nX_m]^{-*}$ which contain three-dimensional delocalized spins. Three-dimensional spins are rare for carbon compounds, except in the case of fullerenes. Bridging these two classes of compounds are the carborane radicals.

5.1 Boron-carbon radicals

The synthesis, characterization, and electrochemistry of the electron deficient *tris*(aryl)boranes $B(C_6F_5)_3$ - $n(C_6Cl_5)_n$ ($n = 1-3$) was reported.⁶² In contrast to previous work done in THF, better voltammetric results were obtained in CH_2Cl_2 . For each borane, a single reduction process is observed; the re-oxidation wave is scan-rate dependent and the behaviour is consistent with an *EC* mechanism. The mid-point potentials for reduction shift to less negative values with increasing n as follows: $-2.0(1)$, $-1.87(5)$, $-1.55(5)$ and $-1.48(2)$ V vs. $Fc^{0/+}$ using 0.1 M $[^nBu_4N][BF_4]$ or 0.1 M $[^nBu_4N][B(C_6H_3(CF_3)_2)_4]$ in CH_2Cl_2 . The EPR spectrum of $B(C_6Cl_5)_3^{-*}$ was measured in blue solutions from sodium reduction in THF and it was shown to have a half-life of 115 min at 298 K, considerably more stable than the ~ 2 min previously reported for $B(C_6F_5)_3^{-*}$. The spectrum is a 1:1:1:1 quartet ($g = 2.002$) from the dominant ^{11}B isotope with $a(^{11}B) = 1.03$ mT with broad, distinctly Gaussian lines (estimated LW ~ 0.5 mT) indicative of substantial unresolved coupling. This work substantiates previous estimates for the reduction potential of $B(C_6F_5)_3$ obtained from an extrapolation.⁶³

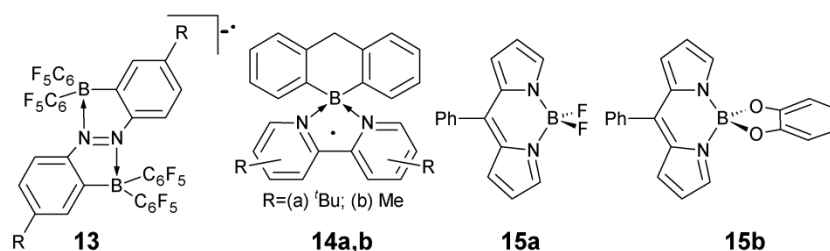
1-Ferrocenyl-2,3,4,5-tetraphenylborole was investigated by CV, showing a single irreversible oxidation process (nominally $Fe^{II/III}$), but two reduction processes with the first quasi-reversible process centred at $E^0_{1/2} = -1.96$ V vs. $Fc^{0/+}$ indicating the formation of stable borole radical anion, **9**.⁶⁴ A second reduction occurs at -2.7 V and is much less reversible. The EPR spectrum of **9** in THF at 200K shows a broad 1:1:1:1 quartet dominated by coupling to ^{11}B , $a(^{11}B) = 0.373$ mT. The radical can be isolated as its $K(THF)_2$ salt. More recently, the same group has managed to isolate and crystallographically characterize a pentaaryl borole radical, 1-mesityl-2,3,4,5-tetraphenylborole, **10**, as an uncoordinated free anion radical using Cp_2Co as reducing agent.⁶⁵ It is reduced reversibly ($E^0_{1/2} = -1.69$ V vs. $Fc^{0/+}$) and also has a second, irreversible reduction at much lower potential ($E_p^c = -2.54$ V). The EPR spectrum of a chemically reduced sample shows four rather broad Gaussian lines (LW ~ 0.27 mT) of equal intensity ratio ($g = 2.0025$) with $a(^{11}B) = 0.343$ mT.

Use of CAAC-carbenes affords stabilization of borylene, HB, which, in marked contrast to the well-known tricoordinate boron(+3) derivatives, features boron in the +1 oxidation state.⁶⁶ *Ab initio* calculations show that the HOMO of the borane is essentially an electron pair in the $p(\pi)$ -orbital of boron so that, in contrast to classical boranes which are the archetypal Lewis acids, the borylene complex is a Lewis base and is isoelectronic with amines. This electron-rich species then, as mentioned in Section 1, is readily oxidized to give the radical cation **11**.



With a single NHC, conventional carbene-borane adducts $R_2C: \rightarrow BH_3$ complexes form, but here too the electron-rich nature of the complexes facilitates H abstraction reactions that generate stable radicals.⁶⁷ EPR spectroscopic data, coupled with DFT computations, demonstrates that the $NHC-BH_2^*$ radicals are planar π -delocalized species. Replacement of one hydrogen at boron by organic groups affords very similar NHC complexes that also undergo hydrogen abstraction to give radicals such as **12**.⁶⁸ Fifteen of such “second-generation” NHC-ligated boranes with aryl and alkyl substituents on boron were prepared, and their radical chemistry was explored by electron paramagnetic resonance (EPR) spectroscopy and DFT calculations. The $NHC \rightarrow BHAr^*$ boryl radicals are akin to diphenylmethyl radicals with the unpaired spin extensively delocalized across the NHC, BH, and aryl units; their reactivity has been extensively investigated.

A series of diborylazobenzenes **13** has been prepared as fluorescent dyes ($R = H, ^nBu, Br, O^nBu$). The electrochemical properties of these species was investigated by CV.⁶⁹ The cyclic voltammogram of (*E*)-**13** ($R = H$) exhibits a facile reversible reduction wave at $E_{1/2} = -0.13$ V ($E_p^c - E_p^a = 80$ mV) vs. Ag/Ag^+ in CH_2Cl_2 (+0.52 V vs. $Fc^{0/+}$), while (*E*)-**13** ($R = ^nBu$) exhibits a similar reversible reduction wave [$E_{1/2} = -0.28$ V (+0.39 V vs. $Fc^{0/+}$)]. The EPR spectrum of the anion radical **13** ($R = ^nBu$) displays a broad singlet with $g = 2.0037$. Reduction quenches the azobenzene fluorescence but this can be restored by air oxidation, thus providing a potential method for switching/sensing.



A fine example of multi-mode spectroelectrochemical investigation was reported for a polyaniline boronic acid which makes use of the Neudeck and Kress style optically semi-transparent EPR/UVvis spectroelectrochemical cell.¹⁸ The boron centre enables a unique self-doping mechanism for this material that differs from the conventional mechanism for sulfonic acid, carboxylic acid and phosphoric acid substituted polyanilines. This self-doping involves the formation of four-coordinate boronate species in the presence of Lewis bases including carbohydrates, vitamins, coenzymes and ribonucleic acids as well as alcohols and fluoride.

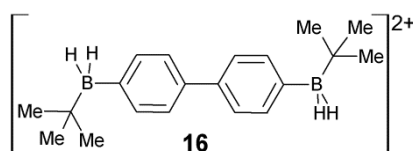
5.2 Boron-nitrogen radicals

The persistent radical $[BCl_2(bipy)]^*$ (bipy = 2,2'-bipyridyl), has been prepared and characterised by X-ray crystallography, EPR and DFT calculations.⁷⁰ The EPR spectrum in toluene exhibits a multiline spectrum; of 11340 theoretical lines, only about 150 are resolved. This EPR spectrum is consistent with a bipy-centred radical. Calculations indicate only 0.15% spin density on boron corresponding to $a(^{11}B) = 0.37$ mT. Interestingly this is very similar to the experimental HFS confirmed from a simulation of the spirocyclic boron radical **4a**.¹⁰ Closely related spirocyclic boronium ions based on the 9-bora-9,10-dihydroanthracene scaffold and substituted 2,2'-bipyridyl ligands have been prepared; these cations are shown to be convenient starting materials for the preparation of neutral radicals **14a,b**.⁷¹ The EPR spectra of the radicals are also multi-line indicative of a bipy-centred radical and to their credit these workers, unlike Mansell *et al.*, succeeded with full simulations using a combination of DFT calculated HFS and iterative line-fitting. Curiously, however, their claim to have “significant

spin density on boron" (never quantified in the paper) seems out of line with the HFS to boron, $a(^{11}\text{B}) = 0.3891$ and 0.4358 mT for **14a** and **14b**, respectively which are really very similar to that found in $[\text{BCl}_2(\text{bipy})]^*$ and **4a**.

As a final example of tetrahedral boron-nitrogen radicals, the 5-(phenyl)dipyrrin (BODIPY) complexes with either BF_2 **15a** or a boron catechol complex **15b** have been prepared and shown to undergo reduction to the corresponding anion radicals.⁷² The reversible one-electron (proven by coulometry) reductions occur at -1.15 V and -1.11 V vs. $\text{Fc}^{0/+}$ and complex multi-line EPR spectra ($g = 2.0029, 2.0027$ respectively) were obtained by X-band EPR spectroscopy in fluid solutions. Here, just as Mansell *et al.*, the authors claim to have been unable to simulate the multi-line EPR spectra. Note that effective strategies for the simulation of such complex ligand-centred spectra of main group radicals have been developed.^{73,74}

The first example in which 4,4'-bipyridyl is quaternised by two boronium ions $[\text{BH}_2\text{NMe}_3]^+$ shows that the resulting "boroviologen" **16** (as the iodide salt) is 0.19 V more difficult to reduce than methyl viologen in aqueous solution containing KCl as electrolyte.⁷⁵ Thus quaternisation of 4,4'-bipy with boronium units constitutes the most effective means found to date for shifting viologen reduction potentials to more negative values while retaining chemical stability. No EPR spectrum is reported and spectroelectrochemistry failed because of a strong tendency to deposit on electrode surfaces.

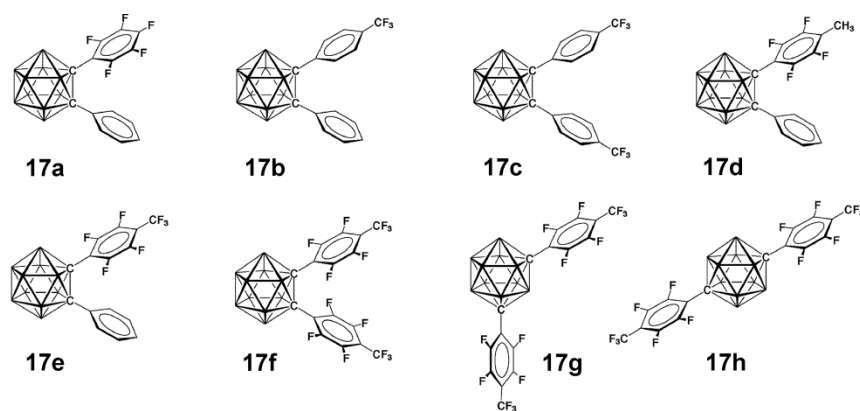


5.3 Polyhedral borane and carborane radicals

The synthesis and isolation of $[\text{B}_{12}\text{Cl}_{12}]^*$ and a study of the $[\text{B}_{12}\text{X}_{12}]^{-2/-\bullet/0}$ redox series by CV in both CH_3CN and the exotic solvent $\text{SO}_2(l)$ has been reported.⁷⁶ The EPR spectrum of $[\text{B}_{12}\text{Cl}_{12}]^*$ is a featureless singlet due to the many overlapping isotope lines, as is common for polyhedral borane radicals. A large prospective study of the redox energetics for *hypercloso* boron hydrides B_nH_n ($n = 6 - 13$) and $\text{B}_{12}\text{X}_{12}$ ($\text{X} = \text{F}, \text{Cl}, \text{OH}$ and CH_3) has been undertaken by computational methods.⁷⁷ The calculated redox energies are compared with all the extant experimental electrochemical data. This very useful and thorough study has indicated some questionable experimental data that need to be re-investigated. The improvements in the potential data recently reported for $\text{B}_{12}\text{X}_{12}$ ($\text{X} = \text{F}, \text{Cl}$) in SO_2 by ⁷⁶ is particularly noted in this article. $[\text{Closo-B}_{12}\text{H}_{12}]^{2-}$ undergoes oxidative perhydroxylation to the stable inorganic cluster redox system $[\text{B}_{12}(\text{OH})_{12}]^{2-\bullet}$.⁷⁸ The air stable, paramagnetic, sparingly water-soluble, solvent-free radical compound $\text{Cs}[\text{B}_{12}(\text{OH})_{12}]$ can be synthesized directly through perhydroxylation of $\text{Cs}_2[\text{B}_{12}\text{H}_{12}]$ with H_2O_2 (30%) at 65°C for six days. The radical anion exhibits an unresolved EPR signal at $g = 2.0042$ (LW = 2.5 mT) in the solid, which is close to the free-electron value of 2.0023 and not much different from the value of 2.0076 for $[\text{hypocloso-B}_{12}\text{Me}_{12}]^*$.

The synthesis spectroelectrochemistry of eight new icosahedral carboranes bearing fluorinated aryl groups has been reported.⁷⁹ An EPR study of the electrogenerated monoanions from the *ortho*-carboranes **17a-f** confirms the cage-centred nature of the redox processes. In contrast, the reduction of the *meta*- and *para*-carboranes **17g,h** appears to be centred on the aromatic substituents, a conclusion supported by the results of DFT calculations. For **17a-f**, the paramagnetic features are typical of an $S = \frac{1}{2}$ system with $g = 2.002$. No evidence for hyperfine or superhyperfine coupling with magnetically active nuclei (^1H , ^{19}F , ^{10}B or ^{11}B) was detected. The linewidth and the g value ($g = 2.004$) confirm the radical character of the monoanion as well as the complete

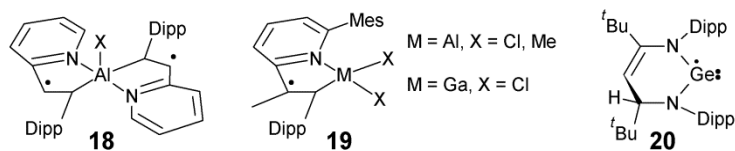
delocalisation of the extra electron inside the carborane cage. **17g,h** display irreversible voltammograms and do not show EPR spectra for radical cations.



6 Aluminium → Indium

The reaction of ground-state Al atoms with dichloromethane (CH_2Cl_2) in an adamantane matrix at 77 K yields two mononuclear Al species.⁸⁰ The magnetic parameters of the main Al-containing product (axial EPR spectrum with $g_{11} = 2.0037(3)$, $g_{22,33} = 2.0030(3)$, $A_1(^{27}\text{Al}) = 1307(1)$ MHz, $A_{2,3}(^{27}\text{Al}) = 1273(1)$ MHz, $A(^{35}\text{Cl}) = 34(1)$ MHz and $A(^{37}\text{Cl}) = 28(1)$) were assigned to the Al-atom insertion product, $\text{ClCH}_2\text{AlCl}^*$ in its *gauche* conformer by sophisticated DFT calculations. The minor product has a similar spectrum with about 15% smaller ^{27}Al HFCs which fits calculations either for the *anti*-conformer or for an adduct with a donor molecule (such as water). A large amount of CHCl_2^* radical is also produced under the reaction conditions.

A detailed study has been undertaken of six complexes of Al(III) with 2,6-bis(isopropyl)-*N*-(2-pyridinylmethylene)phenylamine, IP, which show multiple oxidation states via ligand redox activity.⁸¹ Of particular interest is the neutral L_2AlCl complex **18**, which forms a ligand-centred biradical. EPR spectroscopy measurements confirm the ligand-based biradical, and antiferromagnetic coupling at low temperature is proposed for **18** based on variable temperature magnetic susceptibility measurements. The 100 K X-band CW-EPR spectrum of a dilute frozen solution of **18** features a pattern consisting of four lines between 310 and 360 mT characteristic of a triplet state ($S = 1$) as well as a single line due to a doublet species ($S = 1/2$). Both signals show a typical g value of 2.004(1) for carbon/nitrogen-centred delocalized organic radicals. The triplet nature of the four-line spectrum is confirmed by the additional presence of a weak $\Delta m_S = \pm 2$ transition at half field. By contrast, The mixed-valent, monoradical complex $(\text{IP}^-)(\text{IP}^{2-})\text{Al}^*$ is unstable toward C–C coupling, and the corresponding dimeric complex has been isolated. More recently, these workers show that when $X = \text{OH}$, ligand-based oxidation makes the AlO centre active at C–H bond activation.⁸² The tendency towards dimerization can be overcome by further substitution of the ligand and recently this same group has reported the isolation of monomeric MCl_2 or $\text{M}(\text{CH}_3)_2$ radicals **19** with Al and Ga.⁸³ These radicals have not, however, been characterized by EPR spectroscopy.



7 Carbon

Organic radicals have attracted much attention from the viewpoints of not only synthetic chemistry but also materials science. Very useful reviews of several aspects of carbon-centred radicals are found in the book by Hicks,¹ including triarylmethyl radicals,^{84,85} phenalenyls, fullerenes, carbon nanotubes.⁸⁶ By its focus on materials applications, the coverage does a good job of bringing together the organic and MG inorganic interests in stable radicals.

7.1 Open-shell carbon-rich materials

EPR spectroscopy has been applied to graphitic materials that are heavily fluorinated for application as rechargeable battery materials which display enhanced electrochemical performance.⁸⁷ EPR detected dangling bonds in the post-fluorinated materials. A detailed *in situ* EPR/UV-Vis-NIR spectroelectrochemical study of the oligothiophene/single walled carbon nanotube (SWCNT) interface has been published which provides insight into the interaction of nanotubes with oligothiophenes.⁸⁸ EPR spectra were obtained that are close to isotropic in appearance, indicating that the attached 6-oligothiophene moieties have close to free motion. The link between isolated phenalenyl radicals and open shell graphene materials has been stressed in a recent “perspectives” article.⁸⁹

7.2 Open-shell fullerenes

A family of highly stable (poly)perfluoroalkylated metallic nitride cluster fullerenes was prepared in high temperature reactions and characterized by spectroscopic methods including EPR, structural and electrochemical methods.⁹⁰ Electrochemical studies revealed that $\text{Sc}_3\text{N@C}_{80}(\text{CF}_3)_n$ derivatives are easier to reduce than $\text{Sc}_3\text{N@C}_{80}$, the shift of $E_{1/2}$ potentials ranging from +0.11 V ($n = 2$) to +0.42 V ($n = 10$). Stable radical anions of $\text{Sc}_3\text{N@C}_{80}(\text{CF}_3)_n$ were generated in solution and characterized by EPR spectroscopy, revealing ^{45}Sc hyperfine structures which clearly point to fixed positions of the triangular NSc_3 clusters w.r.t. the fullerene wall. The spectrum of $[\text{Sc}_3\text{N@C}_{80}(\text{CF}_3)]_{10}^{\bullet-}$, $g = 2.0009$, fits well to $a(^{45}\text{Sc}) = 0.06, 1.11, \text{ and } 2.15$ mT and $\text{LW} = 0.19$ mT, whereas the spectrum of $[\text{Sc}_3\text{N@C}_{80}(\text{CF}_3)]_{12}^{\bullet-}$, $g = 2.0012$, fits to $a(^{45}\text{Sc}) = 0.06, 0.74, \text{ and } 0.81$ mT and $\text{LW} = 0.22$ mT.

8 Silicon → Lead

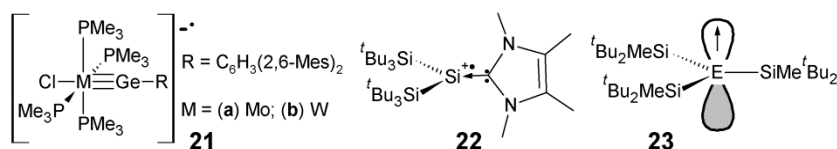
The field of heavy Group 14 radicals has been particularly fertile during the review period with the number of published papers exceeded only by the prodigious nitrogen chalcogenide heterocyclic radicals. Konu and Chivers provide an excellent introduction to this field in the book chapter on stable radicals of the heavy *p*-block radicals.⁹¹ Other recent reviews include those by Power⁹² and Sekiguchi.^{93,94}

8.1 Two-coordinate Si, Ge, Sn or Pb radicals

Stoichiometric reduction of the bulky β -diketiminato germanium(II) chloride complex $[\{\text{N}(\text{Dipp})\text{C}(\text{tBu})\}_2\text{CH}\text{GeCl}]$, $\text{Dipp} = 2,6\text{-}^i\text{Pr}_2\text{C}_6\text{H}_3^-$, with reducing agents such as sodium naphthalenide afforded the radical **20** in moderate yields.⁹⁵ X-ray crystallographic, EPR/ENDOR spectroscopic, computational, and reactivity studies revealed this to be the first authenticated monomeric, neutral germanium(I) radical. The X-band EPR spectrum has slightly rhombic symmetry with $g_{11} = 1.968$, $g_{22} = 1.997$, $g_{33} = 2.001$, and $g_{\text{iso}} = 1.988$, hfc to the ^{73}Ge nucleus was observed in the spectrum and satisfactorily simulated using the values $A_{11} = 82.5$ MHz, $A_{22} = 37.5$ MHz, and A_{33}

= 42.0 MHz (signs not determined). DFT calculations, regardless of the functional used, indicate that the spin density in **20** is predominantly centred on Ge (84.9% - 91.2%) with little delocalization on to the NCCCN backbone of the ligand.

Certain new molybdenum and tungsten germylene complexes, which have formal $M\equiv Ge$ triple bonds, have been shown by CV to undergo reversible one-electron reductions.⁹⁶ The products from chemical reduction in the same potential range are unprecedented germanium analogues of open-shell alkylidyne complexes which have EPR signals that can be analysed to show 17% (Mo) and 12% (W) spin density on the Ge atom. The $E_{1/2}$ values are -0.87 (Mo) and -0.91 V (W) on the $Fc^{0/+}$ scale (though measured against Fc^* in 0.1 M $(NBu_4)PF_6/C_6H_5F$). The EPR spectrum of **21a** shows significant g anisotropy ($g_{11} = 2.090$, $g_{22} = 2.060$ and $g_{33} = 1.970$). Complex **21b** shows an even larger g anisotropy with $g_{11} = 2.194$, $g_{22} = 2.160$, $g_{33} = 1.900$. The observed HFS to ^{31}P (**21a**: $a_{11} = 3.2$ mT, $a_{22} = 3.2$ mT, $a_{33} = 3.2$ mT; **21b**: $a_{11} = 3.0$ mT, $a_{22} = 3.7$ mT, and $a_{33} = 3.8$ mT) compare well with the calculated values, which are negative and range from -2.8 mT to -3.9 mT.



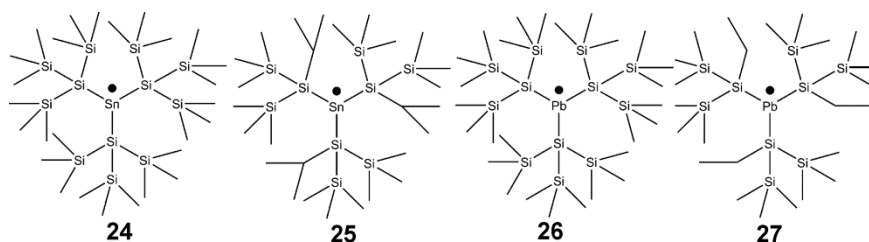
8.2 Three-coordinate Si, Ge, Sn or Pb radicals

An NHC-stabilized silylene radical cation, **22**, has been isolated and characterized by EPR spectroscopy.⁹⁷ The EPR spectrum shows a quintet at a g value of 2.00466 because of coupling with the two ^{14}N nuclei with HFS of $a(^{14}N) = 0.26$ mT, and with weak satellite signals from HFS $a(^{29}Si) = 7.16$ mT. This can be assigned to the coupling with the central three-coordinate Si nucleus and is in the range expected for a planar or close-to-planar silicon which fits with the crystallographic evidence.

Given the long history of triarylmethyl radicals in organic chemistry, analogues amongst the heavier Group 14 elements would be expected; although there is some earlier spectroscopic evidence for such species, the successful isolation and structural characterization of the first (and as yet only) stable triarylgermyl radical $[Ge(3,5-^tBu_2-2,6-(EtO)_2C_6H)_3]^*$ was reported just three years ago.⁹⁸ In the solid state, it has an almost planar geometry at germanium. The frozen solution EPR spectrum obtained on this compound is axial with $g_{11} = 2.004(1)$ and $g_{22,33} = 2.012(1)$ and with HFS of $a(^{73}Ge)_{11} = 8.07$ mT, $a(^{73}Ge)_{22,33} = 4.39$ mT. The majority of the spin density (72 %) is on the ^{73}Ge p orbital. In solution, slightly higher HFS is consistent with calculations that show a slightly pyramidal geometry favoured by 8.5 $kJ\cdot mol^{-2}$.

Whereas Ar_3E^* radicals are scarce, tremendous advances have been made by employing “super” or “hyper” silyl, germyl or silyl/germyl groups *L as substituents* on other Group 14 elements including even carbon itself. Such radicals may be planar with the unpaired spin in an element p orbital and consequently rather small s spin density, especially with very bulky substituents such as for example **23**, or substantially pyramidal as is the case of L_2EH^* radicals.⁹⁹ With their large nuclear g values, even planar species have spectra with substantial HFS values when $E = Sn, Pb$ in complexes such as **24** to **27** where the substituents are polysilyl groups.¹⁰⁰ For the six Pb and three Sn centred radicals reported in this paper, $a(^{207}Pb)$ values range from 79.1 to 125.8 mT (g from 2.039 to 2.105) and $a(^{119}Sn)$ from 39.8 to 62.4 (g from 2.042 to 2.055). Slow tumbling effects in solution result in highly asymmetric line shapes; in the case of some of the plumblyl radicals, the high field line was too broad

to observe. There are simply too many examples of this now prevalent class of radicals to include all the divergent structures or EPR data in this review; readers are urged to consult the references supplied.



The electrochemistry of $({}^t\text{Bu}_2\text{MeSi})_3\text{E}^\bullet$ ($\text{E}=\text{Si}, \text{Ge}, \text{Sn}$) has been investigated and found to show both oxidation and reduction at accessible potentials, none of which are fully reversible.¹⁰¹ Both oxidations and reductions are observed. There is considerably greater dependence of the element type for the oxidations than for the reductions. Oxidations have also been investigated in the gas phase by way of ultra-violet photoelectron spectroscopy.¹⁰² Sequential substituents, in which the atom of attachment to Sn or Pb is Ge, with the latter further substituted with alkylsilyl groups, have been used effectively for a series of tin and lead $\text{L}_3\text{E}^\bullet$ radicals.¹⁰³ An interesting application of this class of radical is the stabilization of interactions with dinitrogen co-dissolved in the media.¹⁰⁴ The hyperfine sublevel correlation spectroscopy (HYSCORE) technique reveals weak but distinct interactions between these main group element radicals and physically dissolved dinitrogen in solution.

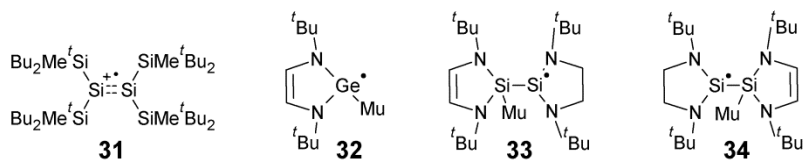
A novel flow-through four-electrode EPR spectroelectrochemical cell used to study reactive $\text{R}_3\text{Si}^\bullet$ radicals was mentioned in Section 2.²¹ With this tool, the authors were able to determine solution-phase EPR spectra of such short-lived species. Precursors such as Ph_3SiCl or Et_3SiCl undergo “preparative” electrolysis resulting in Ph_3Si^- or Et_3Si^- anions formed in solution. In the second stage, the anions are oxidized in a zone under reverse bias to generate short-lived $\text{Ph}_3\text{Si}^\bullet$ or $\text{Et}_3\text{Si}^\bullet$ radicals in the centre of the EPR resonance cavity for either direct detection or spin trapping with phenyl-*N*-tertbutylnitron (PBN).



Photo-reactive polysilyl radicals $({}^t\text{Bu}_2\text{MeSi})_2\text{HSi}-({}^t\text{Bu}_2\text{MeSi})_2\text{Si}^\bullet$ **28** and the previously known $({}^t\text{Bu}_2\text{MeSi})_3\text{Si}^\bullet$ are made in high yields by reduction of Si-Cl bonds with a silyl lithium reagent.¹⁰⁵ The EPR spectrum of the former (290 K, hexane) shows HFS of $a(^{29}\text{Si}^\alpha) = 5.93$; $a(^{29}\text{Si}^\beta) = 0.73$ G; $a(^{29}\text{Si}^\gamma) = 1.04$ mT; $g = 2.0051$. The radicals are susceptible to UV Si-Si bond scission photochemistry. The synthesis and EPR characterization of the 1,3-benzobridged disilyl radical **29** has been reported.¹⁰⁶ The EPR spectrum measured at 80 K in frozen 3-methylpentane shows characteristic signals with a g value of 2.0034. Because it is a triplet biradical, the signal is split into six lines from the magnetic dipole-dipole interaction between unpaired electrons (zero-field splitting, ZFS, parameters $D = 13.8$ mT and $E = 1.72$ mT). By contrast, the isomeric 1,4-species **30** shows quinoidal character and is diamagnetic.

The first isolable cation radical of a bulky disilene was recently reported.¹⁰⁷ Disilenes with a Si=Si double bond are known to readily undergo oxidation or reduction because of their high-lying HOMOs and low-lying LUMOs compared with those of the corresponding alkene analogues, which makes possible the construction of a one-electron reversible redox system. The EPR spectrum of **31** measured at 298 to 200 K in fluorobenzene solutions

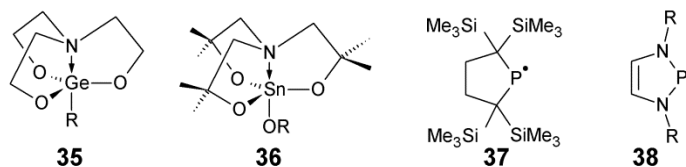
shows a strong signal with a g value of 2.0049, accompanied by a pair of satellite signals (2.30 mT) due to coupling of the unpaired electron with the central ^{29}Si nuclei. The magnitude of the observed ^{29}Si HFS is less than half that of the similar per(silyl)silyl radical ($^t\text{Bu}_2\text{MeSi}$) $_3\text{Si}^\bullet$ (5.80 mT), consistent with delocalization of the unpaired electron over both silicon nuclei in **31**. In a closely related report, it was shown that the 2,4,6-triisopropylphenyl-substituted $\text{R}_2\text{E}=\text{ER}_2$ and $\text{R}_2\text{E}=\text{E}(\text{R})-(\text{R})\text{E}=\text{ER}_2$ ($\text{E} = \text{Si}, \text{Ge}$) undergo well defined oxidation processes under CV conditions with the ease of oxidation of $\text{R}_2\text{Si}=\text{Si}(\text{R})-(\text{R})\text{Si}=\text{SiR}_2 > \text{R}_2\text{Ge}=\text{Ge}(\text{R})-(\text{R})\text{Ge}=\text{GeR}_2 > \text{R}_2\text{Ge}=\text{GeR}_2 > \text{R}_2\text{Si}=\text{SiR}_2$.¹⁰⁸



The final example of a disilyl radical was obtained when certain N-heterocyclic silylenes and germynes were muoniated (muonium, $\text{Mu} = [\mu^+\text{e}^-]$, is an analogue of the hydrogen atom).¹⁰⁹ The resulting muoniated free-radical products were characterized with muon spin resonance (μSR) spectroscopy. While the germylene developed a spectrum consistent with the intended monomeric species **32**, the two silylene muon radicals gave μSR spectra consistent with the dimers from rapid radical coupling reactions with structures **33** and **34**.

8.4 Higher-coordinate radicals of Si, Ge, Sn or Pb

An *in situ* EPR spectroelectrochemical study on radicals produced under reversible electrochemical oxidation of a series of aryl and benzyl germatranes **35** was undertaken.¹¹⁰ A very remarkable feature of the cation radicals of aryl germatranes is that the atrane nitrogen is practically planar as shown by HFS of $a(^{14}\text{N}) = 1.8 - 1.9$ mT. On the other hand, the closely related benzyl radical cations produce EPR spectra consistent with spin localization on the benzyl-Ge portions of the molecules. A very similar stannatrane **36** with a bulky aryl alkoxy substituent undergoes oxidation to a cation radical for which the EPR spectrum fits best for most of the spin density residing on the aryloxy ring and small ^{119}Sn HFS of 0.67 mT.¹¹¹



9 Phosphorus radicals

Activity on phosphorus radicals also remains very lively; a short overview of this vast topic dealing with both neutral and charged species is provided by Konu and Chivers.⁹¹

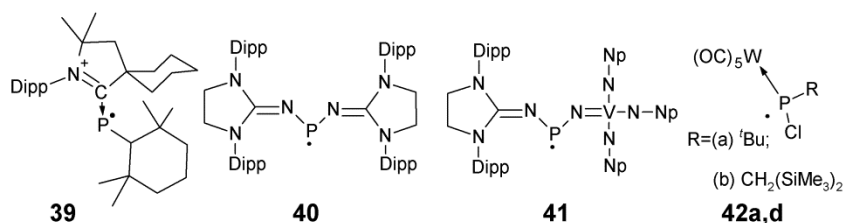
9.1 Stabilization of phosphanyl (two-coordinate) phosphorus radicals

The first fully stable diphosphanyl that is not stabilized by delocalization onto directly attached nitrogen atoms, 2,2,5,5-tetrakis-(trimethylsilyl)-1-phosphacyclopentane-1-yl **37**, has been isolated as air-sensitive yellow crystals.¹¹² The strong tendency of phosphanyls to dimerise to diphosphanes was suppressed by employing these so-called "helmet supersilyl" alkyl groups. The EPR spectrum of **37** in 3-methylpentane at 298 K consists of a doublet signal ($g = 2.0086$) with $a(^{31}\text{P}) = 9.07$ mT and when frozen in the same solvent in an axial spectrum with

$g_{11} = 2.0013$, $g_{22,33} = 2.0084$ and $a_{11}(^{31}\text{P}) = 27.9$ mT, $a_{22,33}(^{31}\text{P}) = 0.49$ mT, which leads to an estimate of 70% and 2% of the spin localized in $3p(\text{P})$ and $3s(\text{P})$ orbitals, respectively.

Novel *N* heterocyclic diphosphanyls dissociate thermally in solution to give the persistent new 7π radicals **38** (^tBu, Mes, Dipp), which are isoelectronic with well-known thiazolyl radicals.¹¹³ The EPR spectrum of **38** (^tBu) recorded at 353 K shows a doublet further split into 1 : 2 : 3 : 2 : 1 quintets ($g = 2.00088$), consistent with hyperfine coupling to one phosphorus [$a(^{31}\text{P}) = 4.1$ mT] and two equivalent nitrogen [$a(^{14}\text{N}) = 0.58$ mT] nuclei. Compared to **37**, the HFS from phosphorus is considerably reduced due to delocalization of the spin over the heterocycle. The crystalline phosphanyl radical **39**, which is stabilized by delocalization onto both nitrogen and a phosphamidine fragment, is thereby rendered indefinitely stable in the solid and in solution in absence of air.¹¹⁴ The fluid solution EPR spectrum ($g = 2.007$) is a doublet of multiplets; the reported $a(^{31}\text{P}) = 9.9$ mT is probably reliable, but the smaller splitting attributed to ^{14}N has not been confirmed by a simulation and indeed seems to be inconsistent with the apparent line width of the reported spectrum. The frozen solution spectrum appears axial with $g_{11} = 2.018$, $g_{22,33} = 2.009$ and $a_{11}(^{31}\text{P}) = 24.7$ mT, $a_{22,33}(^{31}\text{P}) = 2.3$ mT but has excessively broad lines for the axial component. The spin density on the single ^{31}P atom is estimated to be 0.67.

Two more phosphanyl radicals **40** and **41** have been isolated, both stabilized by two nitrogen atoms coordinated to phosphorus, a common theme among stable phosphanyl radicals.¹¹⁵ Whereas **40** is stabilized by two C=N, **41** employs one C=N and one V=N bonds. The latter is found to be the more effective at delocalizing the unpaired electron as shown from the EPR data. For **40**: doublet at $g = 2.005$ phosphorus HFS, $a(^{31}\text{P}) = 7.8$ mT; no coupling with the ^{14}N nuclei was observed; frozen solution: $g_{11} = 2.0074$, $g_{22} = 2.0062$ and $g_{33} = 2.0024$; $a_{11}(^{31}\text{P}) = 24.0$ mT, $a_{22,33}(^{31}\text{P}) = \sim 0$ mT. These results confirm that the spin density is mainly localized in the phosphorus atom with 62% in the $3p(\text{P})$ orbital and about 2% in the $3s(\text{P})$ orbital. For **41**: fluid solution in THF: eight lines pattern at $g = 1.981$, $a(^{51}\text{V}) = 5.8$ mT with no resolved ^{31}P HFS; frozen solution: $g_{11} = 1.9726$, $g_{22} = 2.0048$ and $g_{33} = 1.9583$; $a_{11}(^{51}\text{V}) = 12.1$ mT, $a_{22,33}(^{51}\text{V}) = 3.0$ mT. For this radical, the spin density is mainly localized at the vanadium (67%) and only slightly in the phosphorous $3p$ orbital (1%) as well as on the NHC fragment.

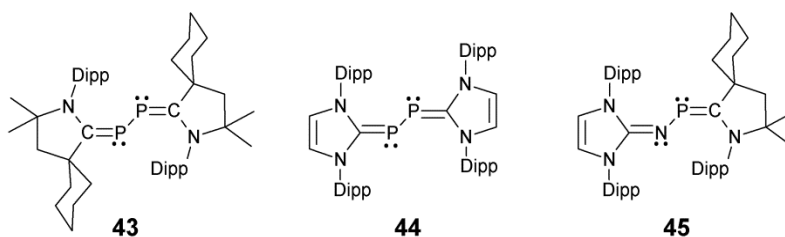


A more traditional way to stabilize reactive low-coordinate phosphorus species is through coordination to a relatively “innocent” $\text{W}(\text{CO})_5$ unit.¹¹⁶ In this way, the transient chlorophosphanyl radicals **42** with a single bulky substituent could be observed by EPR spectroscopy in fluid THF solutions: **42a** $\text{R} = \text{C}_5(\text{CH}_3)_5$ $g = 2.001(2)$; $A(^{31}\text{P}) = 280$ MHz; in frozen solution $A_{11}(^{31}\text{P}) = 560$ MHz, $A_{22,33}(^{31}\text{P}) = -280$ MHz. **42b** $\text{R} = \text{CH}(\text{Si}(\text{CH}_3)_3)_2$ $g = 2.002(2)$; at 150 K $A(^{31}\text{P}) = 137$ MHz; in frozen solution $A_{11}(^{31}\text{P}) = 629$ MHz, $A_{22,33}(^{31}\text{P}) = -314$ MHz. The Mulliken spin populations from DFT calculations at ^{31}P amount to 87% and 82%, respectively.

9.2 Other two-coordinate phosphorus radicals

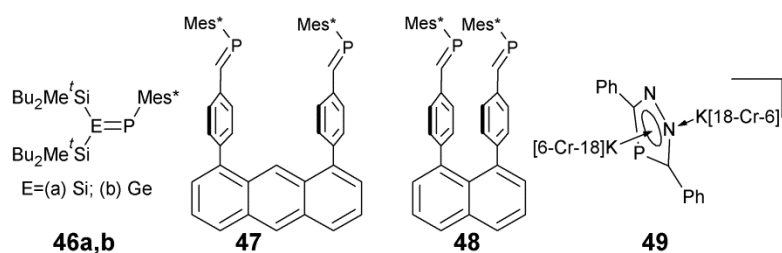
As mentioned in Section 1, singlet carbenes such as NHC and CAACs have been shown to stabilize P_2 fragments.¹¹⁷ These are shown by CV to be extremely electron rich, **43** being reversibly oxidized at $E_{1/2} = -0.536$

V versus $\text{Fc}^{0/+}$ in THF solutions containing 0.1 M $n\text{Bu}_4\text{NPF}_6$ as electrolyte. Incredibly, **44** shows two reversible oxidations, the first at an exceptionally low potential ($E_{1/2} = -1.408$ V versus $\text{Fc}^{0/+}$) as compared to **43** ($\Delta E_{1/2} = 0.872$ V) and the second at $E_{1/2} = -0.178$ V. The room-temperature EPR spectrum of a fluorobenzene solution of **43**^{•+} displays a triplet of quintets ($g = 2.009$) due to coupling with two equivalent phosphorus nuclei ($a(^{31}\text{P}) = 4.2$ mT) and two nitrogen nuclei ($a(^{14}\text{N}) = 0.3$ mT). The frozen solution spectrum shows axial symmetry: $a_{11}(^{31}\text{P}) = 11.7$ mT, and $a_{22,33}(^{31}\text{P})$ close to zero. The EPR spectrum of **44**^{•+} in fluorobenzene solution appears as a broad triplet ($g = 2.008$), $a(^{31}\text{P}) = 4.4$ mT but coupling to N cannot be resolved. In frozen fluorobenzene solution at 100 K, $a_{11}(^{31}\text{P}) = 13.6$ mT.



By using two different carbenes, an NHC on N and a CAAC on P, the reactive “NP” fragment has similarly been stabilized in **45**.¹¹⁸ NP is of interest because it is present in the almost infinite vacuum of the interstellar medium; however, on earth it associates rapidly into higher N_xP_y clusters. One electron oxidation affords the first isolable NP radical cation. The CV of a THF solution of **45**, containing 0.1 M $n\text{Bu}_4\text{NPF}_6$ as electrolyte, shows a reversible one-electron oxidation at $E_{1/2} = -0.51$ V versus $\text{Fc}^{0/+}$, and a second oxidation at about +0.60 V, which is irreversible. The RT EPR spectrum of a fluorobenzene solution of **45**^{•+} displays a doublet owing to a large coupling with phosphorous ($g = 2.0048$; $a(^{31}\text{P}) = 4.4$ mT), surprisingly similar to what is found for **43** and **44** which have two phosphorus nuclei; coupling with the nitrogen atom was not observed which is undoubtedly due to the excessively broad lines in the spectrum, and the much smaller HFS expected for N. In frozen fluorobenzene solution at 100 K a rhombic spectrum is observed with $g_{11} = 2.0028$, $g_{22} = 2.0052$, $g_{33} = 2.0087$ and $a_{11}(^{31}\text{P}) = 14.3$, $a_{22}(^{31}\text{P}) = -1.0$ mT, and $a_{33}(^{31}\text{P}) \approx 0$. The DFT calculated spin density on the single phosphorus nucleus is 0.40.

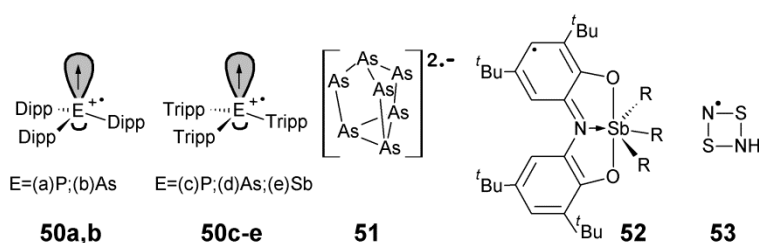
The reactivity of “heavy” phosphalkenes is normally determined by electrophilic character at Si or Ge and nucleophilic at P due to electronegativity differences. By using electron-releasing silyl substituents on Si or Ge and an electron-withdrawing aryl group on P, an attempt has been made to reduce the E=P bond polarity.¹¹⁹ The electrochemical reduction of **46** under CV conditions (vs. Ag/Ag^+ , THF, RT, 0.1 M [$n\text{Bu}_4\text{N}]\text{ClO}_4$) revealed reversible one-electron reduction waves with the reduction potentials $E_{1/2} = -1.78$ V (Si) and $E_{1/2} = -1.75$ V (Ge) [$E_{1/2} = -1.37$ V vs. $\text{Fc}^{0/+}$ (Si) and $E_{1/2} = -1.34$ V vs. $\text{Fc}^{0/+}$ (Ge)]. Interestingly, these values are approximately midway between those of $(t\text{Bu}_2\text{MeSi})_2\text{Si}=\text{Si}(\text{SiMe}t\text{Bu}_2)_2$ (-1.47 V) [-1.06 V vs. $\text{Fc}^{0/+}$] and $\text{Mes}^*\text{P}=\text{PMes}^*$ (-1.93 V) [-1.52 V vs. $\text{Fc}^{0/+}$]. Both anion-radicals were persistent at room temperature, which allowed their characterization by EPR spectroscopy. In THF solution the EPR spectrum of the phosphasilene anion-radical **46a**^{•-} is a doublet with $g = 2.0083$ and $a(^{31}\text{P}) = 5.4$ mT) and silicon satellites with $a(^{29}\text{Si}) = 5.0$ mT. Likewise, the EPR spectrum of the phosphagermene anion-radical **46b**^{•-} contained a doublet resonance with the very characteristic set of 10 satellite signals (^{73}Ge coupling) with the following EPR parameters: $g = 2.0161$, $a(^{31}\text{P}) = 5.6$ mT, $a(^{73}\text{Ge}) = 2.5$ mT.



The radical anions formed when naphthalene and anthracene spacers are used to link two phosphorane moieties in **47** and **48** depend on the nature of the spacer.¹²⁰ The EPR spectra are complex due to orientational motion of the two phosphorane centres w.r.t. each other. EPR spectra indicate that, at room temperature, the electronic structures of the two reduced species **47^{•-}** and **48^{•-}** are quite different. In the former, in good accord with DFT predictions, the unpaired electron is delocalized on the full molecule while in the latter it is confined on a single phosphorane moiety. This difference is attributed to the shorter distance between the two phenylphosphorane groups in **48^{•-}** which hinders their reorientation after addition of an electron. The role of this motion is consistent with the fact that two additional paramagnetic species are detected at 145 K: a di-anion characterized by a rather small exchange-coupling constant from **47** and a radical mono-anion resulting from the formation of a one-electron P–P bond from **48**. The synthesis and CV study of a series of 2-substituted 1,3-benzoxaphospholes and 2,6-substituted benzo[1,2-*d*:4,5-*d'*]bisoxaphospholes has been reported.¹²¹ These compounds are cyclic phosphoranes stabilized by a β ether oxygen. The voltammetry indicates that one-electron reductions are reversible; however, EPR spectroscopic characterization of the putative heterocyclic radicals was apparently not attempted. A potassium crown ether complex (K([18]crown-6)⁺) of a diazaphosphole dianion radical, **49** has been reported.¹²² This radical salt is stable indefinitely in the solid but decomposes slowly in DME or THF solutions. Completely symmetrical EPR signals with large doublet splitting are detected in THF at ambient temperature with $g = 2.0043(1)$ consistent with hyperfine coupling to phosphorus ($a(^{31}\text{P}) = 1.163$ mT). The small value of the HFS is consistent with a π radical.

9.2 Tricoordinate phosphine radical cations

The use of steric shielding from 2,6-diisopropylphenyl groups is now known to render phosphoniumyl radical cations stable and isolable. Thus the radical cations **50** have been prepared as salts with a variety of anions and characterized by EPR spectroscopy.^{123,124} The relatively large HFS of $a(^{31}\text{P}) = 24.1$ mT indicates that the radicals are not entirely planar either in solution or in the solid state. Active work continues on the derivatisation of such radicals by linking the *para* site of one or more aryl rings to redox active groups such as ferrocene, phenothiazyl or naphthoquinone.^{125,126,127}



10 Arsenic → Bismuth

There is a paucity of information on radicals amongst the heavy Group 15 elements. The arsenic and antimony analogues to radical cations **50** have been reported: $\text{Dipp}_3\text{As}^{+\bullet}$ is **50b**;¹²⁸ $\text{Tripp}_3\text{As}^{+\bullet}$ is **50d**; $\text{Tripp}_3\text{Sb}^{+\bullet}$ is **50e**.¹²⁹ Electron deficient clusters of Group 15 elements are rare; thus the report of an electron deficient arsenic Zintl radical anion, $[\text{As}_7]^{2-\bullet}$ **51** is particularly noteworthy.¹³⁰ The CV in DMF/0.1 M LiBF_4 shows a reversible $\text{As}_7^{3-}/\text{As}_7^{2-}$ redox couple. The EPR spectrum ($g = 2.003$) is a broad singlet with HFS showing up in the low temperature spectra (100 K and below; clearest at 5 to 15 K.) The frozen-solution EPR spectra have not yet been analysed in detail. The reactivity of R_2BiX , where R are silyl groups of intermediate steric bulk such as $t\text{-BuPh}_2\text{Si-}$, has been investigated.¹³¹ Reduction of the halides generates polybismuthanes via presumed $\text{R}_2\text{Bi}^\bullet$ radicals. However, the putative radicals have not been observed directly and EPR data has not been obtained to substantiate their existence as intermediates. Electrochemical transformations of antimony (V) complexes containing a tridentate redox-active catecholate ligand, *N,N*-bis-(2-hydroxy-di-3,5-*tert*-butylphenyl)amine, have been reported.¹³² Electrochemical methods are used to generate the neutral secondary radicals **52** (after loss of H^+) from the dianionic catecholate ligand complexes. Their EPR spectra are dominated by the magnetic Sb nuclei, with broad Gaussian lines that obscure the HFS from the ligand nuclei: $g = 2.0034$, $a(^{121}\text{Sb}) = 3.23$ mT, $a(^{123}\text{Sb}) = 1.75$ mT for **52a** (R = Ph) and $g = 2.0032$, $a(^{121}\text{Sb}) = 3.36$, $a(^{123}\text{Sb}) = 1.82$ mT for **52b** (R = Et).

11 Nitrogen chalcogenides

Activity amongst the (poly) nitrogen sulphide and nitrogen selenide radicals, including heterocyclic derivatives, remains very intense. Treatment of this topic commences with binary polythiazyl compounds and then continues with a necessarily terse treatment of the prodigious heterocyclic output. A recent review article provides a brief overview of a new approach to chalcogen–nitrogen heterocyclic π -radicals, particularly 1,2,3- and 1,3,2-benzodithiazolyls, based on thermolysis or photolysis of closed-shell precursors.¹³³ The approach is especially useful for fluorinated radicals. EPR data for 14 examples are analysed in this article by comparison to DFT calculations. Another useful review of stable heterocyclic radicals links organic radicals with poly-N,S radicals that are considered “inorganic”.¹³⁴ The link between poly-N,S radicals and organic materials chemistry is highlighted in another useful review article.¹³⁵ The excellent book chapter by Hicks can be recommended, in particular for the strong emphasis on materials science applications from amongst this family of stable radicals as well as to provide an historical treatment of a vast subject.¹³⁶ Just published is an article that is primarily focussed on materials applications.¹³⁷

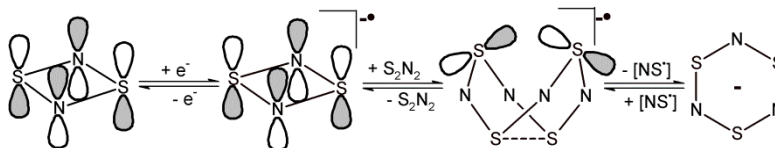
11.1 $\text{N}_3\text{S}_3^\bullet$, the open-shell trimer of NS^\bullet

The neutral 9π -electron ring radical $\text{N}_3\text{S}_3^\bullet$ is an elusive member of the family of binary nitrogen sulphide radicals. Recent exhaustive attempts to generate and detect $\text{N}_3\text{S}_3^\bullet$ by *in situ* electrolytic oxidation of various N_3S_3^- salts at temperatures down to -60 °C failed to detect any EPR signals for this species even though voltammetric evidence for finite concentrations of $\text{N}_3\text{S}_3^\bullet$ was strong.¹⁹ Possible reasons for failure to detect the EPR signal include exchange broadening (that the temperatures investigated fall within a broad coalescence region of the undistorted and second-order Jahn-Teller distorted structures) or that rapid dimerization occurs to $[\text{N}_3\text{S}_3]_2$. Although radical-monomer/diamagnetic-dimer equilibria are known for many nitrogen sulphide hetero-radicals, these usually show strong EPR signals for radicals resulting even from small degrees of dissociation. Alternatively a dimer such as $[\text{N}_3\text{S}_3]_2$ may disproportionate irreversibly to (diamagnetic) N_4S_4 and N_2S_2 . *In situ* EPR-electrochemistry was able to demonstrate the rapid formation of N_4S_4 under conditions where $[\text{N}_3\text{S}_3]^-$ was oxidatively electrolysed. The best kinetic model derived from voltammetry for the interconversion

of N_4S_4 and $N_3S_3^{\bullet}$ in solution proposed a steady state NS^{\bullet} concentration $\sim 20\%$ that of bulk $N_3S_3^-$ and a half-life in solution for $N_3S_3^{\bullet}$ of 0.2 to 0.8 s.¹⁹

11.2 $N_2S_2^{+\bullet}$ cation and $N_2S_2^{-\bullet}$ anion radicals

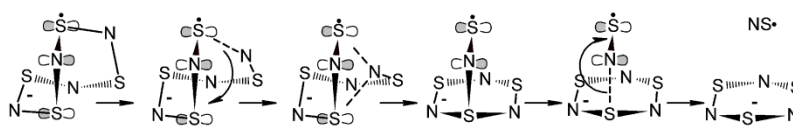
The solution electrochemistry of cyclo-1,3- N_2S_2 has been re-investigated in detail in CH_3CN , CH_2Cl_2 and THF solutions but failed to detect an oxidation process that can be reliably assigned to the formation of the cation radical.¹³⁸ Indeed, the quasi-reversible oxidation process previously reported as the 0/+1 redox couple was observed to occur with $E_m^0 = -0.30, -0.35$ and -0.34 V vs. $Fc^{0/+}$ in these three solvents, which are now known to belong to the $S_3N_3^{-/0}$ redox couple.¹⁹ the origin of this material is likely to be $N_4S_4^{-\bullet}$; the latter is known to decompose rapidly to $S_3N_3^-$ under similar conditions.¹⁹ Cathodic scans indicate a rich reductive voltammetry with an irreversible first reduction occurring at $-1.40, -1.37$ and -1.29 V vs. $Fc^{0/+}$ in the three solvents, respectively. Upon further cathodic scanning, the CV shows continuous current flow, with a second irreversible peak occurring at $-2.18, -2.20$ and -2.25 V in the same solvents. Reversal of the scan direction after traversing either the first or the second cathodic processes shows only the $N_3S_3^{-/0}$ redox couple as mentioned above. These results have been interpreted and kinetically modelled in terms of the rapid dimerization reaction between $N_2S_2^{-\bullet}$ and excess N_2S_2 to form $N_4S_4^{-\bullet}$ in solution (Eqn 2). No EPR signal could be detected from $N_2S_2^{-\bullet}$ due to its very short lifetime; however, protonation from adventitious or deliberately introduced moisture or acid produced strong solution-phase EPR signals attributed to $N_2S_2H^{\bullet}$ **53**: $a(^{14}N_1 = 1.12)$; $a(^{14}N_2 = 0.65)$; $a(^1H = 0.60$ mT); $g = 2.0136(1)$ at -20 °C in CH_3CN . This radical has an estimated half-life in solution of 7(1) s at -70 °C.²¹⁷ Consistent with the mechanism established by electrochemistry, a variety of chemical reducing agents were found to reduce N_2S_2 to salts of $N_3S_3^-$ quantitatively.¹⁹



[2]

11.3 The $N_4S_4^{-\bullet}$ anion radical

EPR spectra from $N_4S_4^{-\bullet}$ detected in an *in situ* EPR-electrochemistry cell at sub-ambient temperatures have been reported for each isotopic species $^{14}N_4^{32}S_4^{-\bullet}$, $^{15}N_4^{32}S_4^{-\bullet}$ and $^{14}N_4^{33}S_4^{-\bullet}$ as part of a detailed re-investigation of the voltammetry of N_4S_4 in a variety of common solvent/electrolyte systems.¹⁹ The measured HFS values at -20 °C in CH_2Cl_2 solution are: $a(^{14}N) = 0.1175$, $a(^{15}N) = 0.1535$ and $a(^{33}S_{1-7}) = 0.20$ mT; $g = 2.0008(1)$. These data are consistent with a rapid exchange process between the two degenerate C_{2v} structures of the anion radical at -20 °C resulting in averaging of the $a(^{33}S)$ HFS values (the calculated average due to the opposite signs of the two values comes to 0.32 mT). This work proposed a mechanism based on detailed digital simulations of the CV data and stoichiometry established from rotated-disk voltammetry and bulk electrolysis. Re-arrangement of the activated $N_4S_4^{-\bullet}$ anion radical occurs through a well-attested 1,3-nitrogen shift reaction followed by expulsion of NS^{\bullet} , the latter rapidly oligomerizing to fresh N_4S_4 (Eqn 3). An Arrhenius activation energy for the first-order decay of $N_4S_4^{-\bullet}$ was measured as 62(2) $\text{kJ}\cdot\text{mol}^{-1}$.



[3]

11.4 Thiadiazolyl anion radicals and congeners

The benzo-2,1,3-thiadiazolyl radical anion **54** has been crystallized with $K(\text{THF})^+$.¹³⁹ The reaction solution revealed an EPR spectrum that was in full agreement with that reported for **54** previously. The experimental HFS constants in THF solution are $a(^{14}\text{N}) = 0.530$, $a(^1\text{H}) = 0.265$, $a(^1\text{H}) = 0.165$ mT.¹⁴⁰ The redox properties and radical anions of a large number of fluorinated 2,1,3-benzothia(selena)diazoles **55** and related compounds have been reported.¹⁴¹ Electrochemical reductions are reported for 11 new derivatives and their EPR parameters have also been determined. Full simulations of these multi-line radical anions were undertaken, lending great credibility to the reported parameters. A recent study reports on the reduction of 3,4-dicyano-1,2,5-thiadiazole and the related selenadiazole,¹⁴² [1,2,5]-thiadiazolo[3,4-c][1,2,5]thiadiazole, [1,2,5]selenadiazolo-[3,4-c][1,2,5]thiadiazole, 3,4-dicyano-1,2,5-thiadiazole, **56a**, and 3,4-dicyano-1,2,5-selenadiazole, **56b**, which have nearly the same positive electron affinity (EA).¹⁴² Under the CV conditions, **56** readily produce long-lived π -delocalized radical anions (π -RAs) characterized by EPR. With thiophenolate (PhS^-) salts they form charge-transfer adducts rather than radicals from full electron transfer.

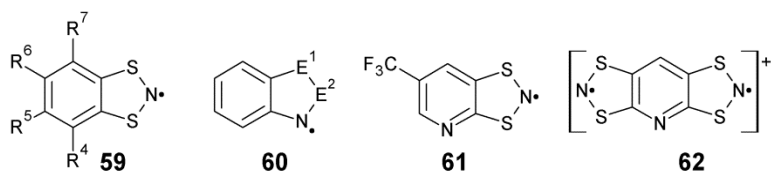


The isolation and structural characterization of the radical monoanion of [1,2,5]thiadiazolo[3,4-c][1,2,5]thiadiazolidyl **57** as a salt with bis(pentamethyl)cyclopentadienylchromium has been reported.¹⁴³ The lack of an EPR spectrum in this salt in either solid or solution phase has been investigated in detail. This unusual non-metal open shell compound is the first example of a heterospin π -heterocyclic radical anion salt.¹⁴³ At ambient temperature, interaction of the solid radical anion salt of **57** $[\text{Na}(15\text{-crown-5})][\text{C}_2\text{N}_4\text{S}_2]$ with water vapour unexpectedly leads to the trithionate salt $[\text{Na}(15\text{-crown-5})]_2[\text{S}(\text{SO}_3)_2]$; it is rare that the product of hydrolysis of a thiazyl radical can be thus identified.¹⁴⁴ Several salts of the radical anion of 1,2,5-thiadiazolo-naphthoquinone have also been reported.¹⁴⁵ The fluid solution EPR spectrum for this novel anion radical are $g = 2.0044$, $a(^{14}\text{N}) = 0.0460$ mT for two equivalent nitrogen atoms, $a(^1\text{H})_1 = 0.1116$ mT for two equivalent hydrogen atoms, and $a(^1\text{H})_2 = 0.0398$ mT for a second set of two equivalent hydrogen atoms.

11.5 Dithiazolyl radicals and congeners

While closely related to the previous class of thiazyl heterocycle, dithia- and diselenazolyls are *neutral* radicals by virtue of replacement of an N by S/Se. There are two isomers which are distinguished by having either an SNS, **59**, or SSN, **60**, sequence. The preparation, crystal structure and magnetism of trifluoromethyl-pyridyl-1,3,2-dithiazolyl **61** has been reported.¹⁴⁶ The steric demand of the TFM group destabilises the dimeric phase previously reported for pyridyl-1,3,2-dithiazolyl thereby driving the formation of a spin transition material. The 3,4-dialkoxybenzo-1,3,2-dithiazolyl radical **59** ($\text{R}^5=\text{R}^6=\text{OCH}_3$) has been prepared for the first time and its structure determined by X-ray crystallography.¹⁴⁷ In fluid solution in THF at 298 K, the EPR spectrum is a typical 1:1:1 triplet, $g = 2.010$, $a(^{14}\text{N}) = 1.11$ mT. Note that the HFS to ^{14}N is considerably larger than in thiadiazolyl

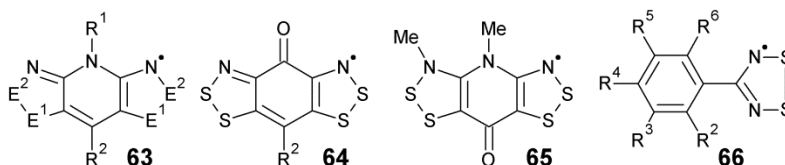
radical anions. Benzo-1,3,2-dithiazolyl **59** ($R^{4,7}=H$) and methylbenzo-1,3,2-dithiazolyl **59** ($R^{4,6,7}=H, R^5=CH_3$) radicals have been incorporated into porous hybrid frameworks via gas phase diffusion.¹⁴⁸ The result revealed that inclusion appeared selective for the flexible coordination polymer, MIL53(Al) (MIL = Materials of Institut Lavoisier), against a range of other potential hosts. The EPR spectrum of the solid inclusion compound shows a broad singlet with MIL53(Al)@MBDTA ($g = 2.0095$, $LW = 0.78$ mT). This is a significant result related to magnetically active framework solids.



New 1,2,3-dithiazolyl (Hertz) radicals **60** have been generated by thermolysis of $R_3P=N$ - derivatives.¹⁴⁹ Complex, multiline EPR spectra, with data extracted from full simulations despite the numerous lines, have been reported for seven radical species **60** with differing combinations of substituents on the benzene ring. A combined pulsed EPR and ENDOR study in frozen $CHCl_3$ solutions at 30 and 80 K has been undertaken for benzo-1,2,3-dithiazolyl **60** ($E^{1,2}=S$) and its possible thiaselenazolyl isomers 1,2,3-thiaselenazolyl **60** ($E^1=S; E^2=Se$); 1,2,3-selenathiazolyl) **60** ($E^1=Se; E^2=S$).¹⁵⁰ These methods, in combination with DFT calculations, were used to study the magnetic parameters of the radicals, namely the principal values of the nitrogen and proton hyperfine interactions and g -tensors. The spin density distribution was shown to be nearly the same for all investigated radicals and, therefore, replacement of sulphur by selenium leads to a limited perturbation of the radicals' electronic structure. A high anisotropy in the g -tensors was found for the selenium-containing radicals.

It has now been shown that cycloaddition of SNS^+ works also for benzo-^{151, 152} and naphthoquinones,¹⁵³ which potentially opens up many new ways to derivatise this ring system. Methods have been developed for calculating the hyperfine coupling and g tensors in this class using DFT and configuration interaction theory.¹⁵⁴ When two SNS or SSN sequences are fused to one ring, the result is usually a singlet state with bond-length alternation in the tricyclic array. Radicals can then be created either by a redox process, as in the following example, or by substitution. A magnetostructural correlation was investigated in three organic radical cation salts based on the monocation of benzo[1,2-d:4,5-d']bis[1,3,2]dithiazolyl **62** (BBDTA), which is an $S = 1/2$ system, and the tetrahedral diamagnetic monoanions, $TlBr_4^-$, TlI_4^- , and InI_4^- , by analysis of their crystal structures and magnetic properties.¹⁵⁵ The preparation, crystal growth, crystal structure, and magnetic properties of three polymorphs (α , β and γ ,) of another organic magnet, BBDTA·GaBr₄, which is also an $S = 1/2$ system, have also been investigated.¹⁵⁶

Substitution of one carbon on the benzo-bridge by nitrogen also affords radicals **63**, but this kind is neutral. A variety of *bis*-1,2,3-dithiazolyl radicals and selenium analogues have been prepared by altering substituents $R^{1,2}$ on the bridging carbon and nitrogen atoms in **63**. The Oakley group has focussed extensively on structure property relationships, including systematic substitution of each S by Se¹⁵⁷⁻¹⁵⁹ and the effect of pressure on the band structure.^{160,161} Recently, ferromagnetic ordering has been discovered in this class of compounds, also affected by the applied pressure.^{12,162-164} The role of multicentre bonding in controlling such magnetic interactions is strongly indicated by structural studies and has also been investigated computationally.¹⁶⁵



Semiquinone-bridged *bisdithiazolyls* **64** represent a new class of resonance-stabilized neutral radical for use in the design of single-component conductive materials.¹⁶⁶ As such, they display electrochemical cell potentials lower than those of related pyridine-bridged *bisdithiazolyls*, a finding which heralds a reduced on-site Coulomb repulsion U . The preparation and structural characterization of the methyl-substituted oxobenzene-bridged *bisdithiazolyl* radical **64a** ($R^2=CH_3$) has been described.¹⁶⁷ This extensively delocalized radical shows two reversible redox processes in CV with $E_{1/2} = -0.557$ and -0.073 V vs. $Fc^{0/+1}$ (CH_3CN , $0.1 M$ nBu_4NPF_6). For the chloro-substituted analogue **64b** ($R^2=Cl$), these values are $E_{1/2} = -0.481$ and -0.195 V vs. $Fc^{0/+1}$.

EPR solutions of **64b**, obtained by dissolving crystals of either unsolvated **64b** or its MeCN adduct in toluene or dichloromethane, display a strong five-line EPR signal reminiscent of that observed for the related nitrogen-bridged radicals **63**. The $a(^{14}N)$ values are approximately one-half of those found in monofunctional 1,2,3-dithiazolyls **60**, as would be expected given the fact that the spin density is distributed evenly between two dithiazolyl rings; $g = 2.0089$, $a(^{14}N) = 0.343$ (x 2); $a(^{35}Cl) = 0.030$ mT.¹⁶⁶ Further investigations of **64c** ($R^2=F$) indicates that with the smaller fluoro substituent, pure crystalline material achieves a metallic state at the modest pressure of 3 GPa.¹⁶⁷

When **63** ($E^1=E^2=S, R^1=Me, R^2=OMe$) is dissolved in CH_2Cl_2 solution, the original spectrum ($g = 2.0087$, $a(^{14}N) = 0.310$ mT for two terminal N, $a(^{14}N) = 0.057$ for the central N and $a(^1H) = 0.031$ for the CH_3 H nuclei) is slowly replaced by a considerably simpler spectrum ($g = 2.0086$, $a(^{14}N) = 0.553$ mT, $a(^{14}N) = 0.048$ mT, each to one N.)¹⁶⁸ The latter spectrum fits very well for the radical **65**, which itself is unstable towards the eventual formation of a zwitterionic pyridine derivative from complete loss of the methyl group originally attached to O.

11.6 Dithiadiazolyl radicals (1,2-DTDA)

Recent reports on monomeric 1,2-DTDA radicals **66** include the magnetic properties of ortho-chlorophenyl substituted radicals **66a,b** ($R^2=Cl; R^5=H, Cl$),¹⁶⁹ the effect on magnetism and low melting temperature when “R” is a long fluorinated tail¹⁷⁰ and several studies on the origin of the famous spin-canted ferromagnetism of some of the polymorphs that form when “R” is 4- XC_6F_4 ($X = CN, NO_2$).¹⁷¹ The synthesis and a crystallographic study of twelve different multifluoro aryl derivatives **66c** ($R^{2-6}=H, F$) has appeared.¹⁷² The EPR spectra of **66a,b** in the crystalline state above 150 K show clear evidence for the presence of a triplet state reflected in (i) additional features attributable to zero-field splitting and (ii) the observation of the forbidden $\Delta M_s = \pm 2$ transition in the half-field region. The spin Hamiltonian parameters for this $S = 1$ species were $g_{11} = 2.002$, $g_{22} = 2.008$, $g_{33} = 2.021$; $|D| = 0.0183$ cm^{-1} , $|E| = 0.0008$ cm^{-1} .¹⁶⁹ Co-sublimation of the two dithiadiazolyl dimeric solids $[PhCNSSN]_2$ and $[C_6F_5CNSSN]_2$ yielded a mixed $\pi^*-\pi^*$ dimer $[PhCNSSN][C_6F_5CNSSN]$ (**3**) exhibiting aryl-perfluoroaryl $\pi-\pi$ interactions.¹⁷³

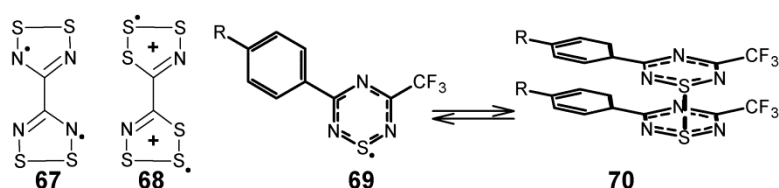
A detailed review of the crystal engineering of the various supramolecular synthons for 1,2-DTDAs, both interacting amongst themselves and with other donor atoms which are normally incorporated on or in the “R” groups belonging to the “RC” moieties, has appeared.¹⁷⁴ The incorporation of 1,2-DTDAs into mesogenic phases has been attempted.¹⁷⁵ A series of liquid-crystalline materials based on 4-substituted cyanobiphenyls,

RC₆H₄C₆H₄CN (R = C₅H₁₁, C₆H₁₃, C₇H₁₅, C₈H₁₇ and C₁₂H₂₅, were functionalised to give the corresponding dithiadiazolyl organic radicals RC₆H₄C₆H₄CN₂S₂•. Temperature-dependent EPR spectra of *n*-C₁₂H₂₅C₆H₄C₆H₄CN₂S₂• reveal that it adopts a dimeric diamagnetic structure in the solid state with a small number of paramagnetic defect sites. At elevated temperatures confined rotational motion is observed, which is associated with rotation about the molecular long axis. This is followed by a reduction in the number of defects through thermal annealing. The dilute nature of the defect sites indicate that this annealing is most likely caused by a radical transfer mechanism. The disjoint diradical 4,4'-bis(1,2,3,5-dithiadiazolyl) **67**¹⁷⁶ has been the object of intensive interest including its use to efficiently harvest an alternating photocurrent¹⁷⁷ and a detailed spectroscopic study of the electronic structures of thin films of this material.¹⁷⁸

A complete picture of the spin density distribution in the organic radical *p*-O₂NC₆F₄CN₂S₂• has been obtained by a combination of polarized neutron diffraction, EPR, and electron-nuclear double resonance (ENDOR) spectroscopies, and DFT calculations.¹⁷⁹ Polarized neutron diffraction revealed that the spin distribution is predominantly localized on the N and S atoms (+0.25 μ(B) and +0.28 μ(B), respectively) of the heterocyclic ring with a small negative spin density on the heterocyclic C atom (-0.06 μ(B)). These spin populations are in excellent agreement with both *ab initio* and DFT calculations (spin populations on the C, N, and S sites of -0.07, 0.22 and 0.31, respectively) and CW-EPR studies which estimated the spin population on the N site as 0.24. The DFT calculated spin density revealed less than 1% spin delocalization onto the perfluoroaryl ring, several orders of magnitude lower than the density on the heterocyclic ring. CW-ENDOR studies at both X-band (9 GHz) and Q-band (34 GHz) frequencies probed the spin populations on the two chemically distinct F atoms. These spin populations on the F atoms *ortho* and *meta* to the dithiadiazolyl ring are of magnitude 10⁻³ and 10⁻⁴, respectively. Resonant ultrasound spectroscopy was used to analyse the elastic and inelastic behaviour associated with canted antiferromagnetic ordering at 36 K in the radical, β-*p*-NCC₆F₄CN₂S₂•.¹⁸⁰ On cooling through the magnetic ordering transition, there is anomalous elastic behaviour away from the expected uniform stiffening with decreasing temperature, consistent with magneto-elastic coupling. The excess in the elastic stiffness follows the magnetic order parameter linearly below the magnetic ordering temperature. A much larger change in elastic properties is associated with short-range ordering between T_c and 150 K, which appears to correlate with an excess heat capacity (and entropy). Thus, it appears that the onset of long-range order to this spin canted system might only be a partial contribution to the whole phase transition.

11.7 1,2,3,4-Trithiazolium cation radicals

The disjoint diradical dication **68** was originally reported in 1993 but the full electronic and magnetic properties were reported recently.¹⁸¹ The disjoint nature of **68** is established by magnetic susceptibility studies of the Sb₂F₁₁ salt doped into an isomorphous diamagnetic host material (CNSNS)₂(Sb₂F₁₁)₂. Intramolecular spin coupling is extremely weak corresponding to a singlet-triplet gap (ΔE_{ST} = 2J) of <|2| cm⁻¹. There is an electronic similarity between **68** and O₂, as the only simple non-sterically hindered non-metal diradicals to retain their paramagnetism in the solid state. In solution the diradical shows a singlet with *g* = 2.0155 and a pentet with *g* = 2.0132, *a*(¹⁴N) = 0.2 mT.



11.8 1,2,4,6-Thiatriazinyl radicals

Recently, a general synthetic route to 3-trifluoromethyl-5-aryl-1 λ^3 -1,2,4,6-thiatriazinyl radicals **69** was developed.¹⁸² Several radicals were crystallographically characterized and exist in the solid state as diffuse π^* - π^* co-facial dimers **70** linked by S...S contacts. The voltammetric behaviour is complex and was interpreted to be indicative of monomer-dimer equilibria in solution. All the EPR spectra are analogous and differ ever so slightly in magnitude with the nature of the remote substituents R. When R = H, $a(^{14}\text{N}) = 0.324, 0.445, 0.425$ mT. Additional HFS is observed to the trifluoromethyl group, $a(^{19}\text{F}) = 0.039$ mT.

11.9 Coordination chemistry of thiazyl radicals

Developments in thiazyl coordination chemistry during the past decade have been thoroughly described in a recent review.¹⁸³ A special focus of the coordination chemistry of thiazyl radicals has been in the design of high-spin coordination complexes.¹⁸⁴ An extensive chemistry occurs when 1,3,2-benzodithiazolyl BDTA is mixed with metal complexes. With cobalt *bis*-maleonitriledithiolate, π -coordination occurs between the heterocyclic ring and the cobalt ion;^{185,186} with the corresponding nickel(II) complex, the DTA interacts with the remote nitrile groups via short N...S interactions;¹⁸⁷ with copper, an almost perfect one-dimensional magnetic material forms,¹⁸⁸ while with Ni(1,3-dithiol-2-thione-4,5-dithiolate)₂, a multiband molecular conductor is obtained.¹⁸⁸ This diverse behaviour has been reviewed.¹⁸⁹

More robust coordination is achieved with 1,2,3,5-dithiadiazolyls modified to bear a 2-pyridyl group attached to the ring backbone such as in **71** ($E^{1,2}=\text{S}$) which enables bidentate coordination similar to that seen in the ubiquitous 2,2'-bipyridyl ligand.¹⁹⁰ More complex ligands have been devised with pyrimidyl groups **72**, which are capable of bridging two M(hfac)₂ units, and benzoxazole groups attached to the ring backbone.¹⁹¹ Secondary donors on the pyridyl group have been employed in attempts to modify crystal packing.¹⁹² A characteristic of this class of metal complexes is that the ligands retain their full open-shell character; in several examples, the magnetic coupling between the metal ion and paramagnetic ligand were readily obtained from solid-state magnetic measurements.



4-(2'-Pyrimidyl)-1,2,3,5-dithiadiazolyl **72a** ($E^{1,2}=\text{S}$) neutral radical ligand and its selenium analogue **72b** ($E^{1,2}=\text{Se}$) act as bridging ligands that enable magnetic communication between two paramagnetic first row transition elements (ML, M = Mn^{II}, Co^{II} or Ni^{II}; L = hfac).¹⁹³ The resulting complexes are robust and volatile such that they can be sublimed in good yield despite their high molecular weight. For the nickel(II) and cobalt(II) complexes of the thiazyl radical **72a**, the magnetic data confirm that the metal-based spin couples ferromagnetically to the ligand-based spin, giving rise to ST = 7/2 and ST = 5/2 spin ground states, respectively. The previously reported manganese(II) complex has a spin ground state ST = 9/2 owing to anti-ferromagnetic coupling between the metal and DTDA spins. However, close intermolecular S...O contacts, albeit disrupted by crystallographic disorder, provide a pathway for intermolecular anti-ferromagnetic coupling between the metal and DTDA spins of neighbouring molecules, giving rise to an increase in the χT product at low temperature.

Acknowledgments

The support of the University of Lethbridge and sponsorship of my research program by the Natural Sciences and Engineering Research Council of Canada is gratefully acknowledged. I am thankful to Dr. Tracey L. Roemmele for assistance with EPR-related research in my laboratory.

References

1. R. G. Hicks, *Stable Radicals: Fundamentals and Applied Aspects of Odd-Electron Compounds*, John Wiley & Sons Ltd., Chichester, 2010.
2. T. Chivers and J. Konu, *Comments Inorg. Chem.*, 2009, **30**, 131.
3. D. Martin, M. Soleilhavoup and G. Bertrand, *Chem. Sci.*, 2011, **2**, 389.
4. D. Martin, M. Melaimi, M. Soleilhavoup and G. Bertrand, *Organometallics*, 2011, **30**, 5304.
5. Y. Z. Wang and G. H. Robinson, *Chem. Commun.*, 2009, 5201.
6. Y. Wang, B. Quillian, P. Wei, C. S. Wannere, Y. Xie, R. B. King, H. F. Schaefer, P. V. Schleyer and G. H. Robinson, *J. Am. Chem. Soc.*, 2007, **129**, 12412.
7. Y. Z. Wang, Y. M. Xie, P. R. Wei, R. B. King, H. F. Schaefer, P. V. Schleyer and G. H. Robinson, *Science*, 2008, **321**, 1069.
8. Y. Z. Wang, Y. M. Xie, P. R. Wei, R. B. King, H. F. Schaefer, P. V. Schleyer and G. H. Robinson, *J. Am. Chem. Soc.*, 2008, **130**, 14970.
9. T. Chivers, D. J. Eisler, C. Fedorchuk, G. Schatte, H. M. Tuononen and R. T. Boeré, *Chem. Commun.*, 2005, 3930.
10. T. Chivers, D. J. Eisler, C. Fedorchuk, G. Schatte, H. M. Tuononen and R. T. Boeré, *Inorg. Chem.*, 2006, **45**, 2119.
11. R. G. Hicks, *Nat. Chem.*, 2011, **3**, 189.
12. K. Lakin, S. M. Winter, L. E. Downie, X. Z. Bao, J. S. Tse, S. Desgreniers, R. A. Secco, P. A. Dube and R. T. Oakley, *J. Am. Chem. Soc.*, 2010, **132**, 16212.
13. S. K. Pal, P. Bag, A. Sarkar, X. L. Chi, M. E. Itkis, F. S. Tham, B. Donnadiou and R. C. Haddon, *J. Am. Chem. Soc.*, 2010, **132**, 17258.
14. N. G. Connelly and W. E. Geiger, *Chem. Rev.*, 1996, **96**, 877.
15. R. T. Boeré, K. H. Mook and M. Parvez, *Z. Anorg. Allg. Chem.*, 1994, **620**, 1589.
16. W. Kaim and J. Fiedler, *Chem. Soc. Rev.*, 2009, **38**, 3373
17. A. Neudeck and L. Kress, *J. Electroanal. Chem.*, 1997, **437**, 141.
18. I. R. Moraes, M. Kalbac, E. Dmitrieva and L. Dunsch, *ChemPhysChem*, 2011, **12**, 2920.
19. R. T. Boeré, T. Chivers, T. L. Roemmele and H. M. Tuononen, *Inorg. Chem.*, 2009, **48**, 7294.
20. P. R. Murray, D. Collison, S. Daff, N. Austin, R. Edge, B. W. Flynn, L. Jack, F. Leroux, E. J. McInnes, A. F. Murray, D. Sells, T. Stevenson, J. Wolowska and L. J. Yellowlees, *J. Magn. Reson.*, 2011, **213**, 206.
21. J. Zeitouny and V. Jouikov, *Phys. Chem. Chem. Phys.*, 2009, **11**, 7161.
22. D. S. Bohle, in *Stable Radicals: Fundamentals and Applied Aspects of Odd-Electron Compounds*, ed. R. G. Hicks, John Wiley & Sons, Ltd, Chichester, 2010, pp. 147.
23. J. Hartung, *Chem. Rev.*, 2009, **109**, 4500.
24. A. Volodin, D. Biglino, Y. Itagaki, M. Shiotani and A. Lund, *Chem. Phys. Lett.*, 2000, **327**, 165.
25. M. Chiesa, E. Giamello and M. Che, *Chem. Rev.*, 2010, **110**, 1320.
26. J. W. Dethlefsen, E. D. Hedegard, R. D. Rimmer, P. C. Ford and A. Dossing, *Inorg. Chem.*, 2009, **48**, 231.
27. R. Lauricella, M. Triquigneaux, C. Andre-Barres, L. Charles and B. Tuccio, *Chem. Commun.*, 2010, **46**, 3675.
28. M. P. Schopfer, J. Wang and K. D. Karlin, *Inorg. Chem.*, 2010, **49**, 6267.
29. M. R. McCarthy, T. J. Crevier, B. Bennett, A. Dehestani and J. M. Mayer, *J. Am. Chem. Soc.*, 2000, **122**, 12391.
30. J. S. Pap, J. L. Snyder, P. M. B. Piccoli and J. F. Berry, *Inorg. Chem.*, 2009, **48**, 9846.
31. I. J. Casely, Y. Suh, J. W. Ziller and W. J. Evans, *Organometallics*, 2010, **29**, 5209.

32. N. A. Siladke, K. R. Meihaus, J. W. Ziller, M. Fang, F. Furche, J. R. Long and W. J. Evans, *J. Am. Chem. Soc.*, 2012, **134**, 1243.
33. M. Wanner, T. Scheiring, W. Kaim, L. D. Slep, L. M. Baraldo, J. A. Olabe, S. Zalis and E. J. Baerends, *Inorg. Chem.*, 2001, **40**, 5704.
34. M. S. Lynch, M. Cheng, B. E. Van Kuiken and M. Khalil, *J. Am. Chem. Soc.*, 2011, **133**, 5255.
35. P. De, T. K. Mondal, S. M. Mobin, B. Sarkar and G. K. Lahiri, *Inorg. Chim. Acta.*, 2010, **363**, 2945.
36. W. M. Irvine, M. Senay, A. J. Lovell, H. E. Matthews, D. McGonagle and R. Meier, *Icarus*, 2000, **143**, 412.
37. P. S. S. Pereira, L. G. M. Macedo and A. S. Pimentel, *J. Phys. Chem. A.*, 2010, **114**, 509.
38. C. F. Leung, D. T. Y. Yiu, W. T. Wong, S. M. Peng and T. C. Lau, *Inorg. Chim. Acta.*, 2009, **362**, 3576.
39. A. Wu, A. Dehestani, E. Saganic, T. J. Crevier, W. Kaminsky, D. E. Cohen and J. M. Mayer, *Inorg. Chim. Acta.*, 2006, **359**, 2842.
40. M. Reinel, T. Hocher, U. Abram and R. Kirmse, *Z. Anorg. Allg. Chem.*, 2003, **629**, 853.
41. X.-Y. Yi, T. C. H. Lam, Y.-K. Sau, Q.-F. Zhang, I. D. Williams and W.-H. Leung, *Inorg. Chem.*, 2007, **46**, 7193.
42. T. Chivers and F. Edelmann, *Polyhedron*, 1986, **5**, 1661.
43. J. R. Dethlefsen, A. Dossing and E. D. Hedegard, *Inorg. Chem.*, 2010, **49**, 8769.
44. J. W. Dethlefsen and A. Dossing, *Inorg. Chim. Acta.*, 2009, **362**, 259.
45. R. Hefferlin, *J. Quant. Spectrosc. Radiat. Transfer*, 2010, **111**, 71.
46. A. Petr, V. Kataev and B. Büchner, *J. Phys. Chem. B*, 2011, **115**, 12036.
47. B. Galliker, R. Kissner, T. Nauser and W. H. Koppenol, *Chem. Eur. J.*, 2009, **15**, 6161.
48. E. Frears, N. Nazhat, D. Blake and M. Symons, *Free Radical Res.*, 1997, **27**, 31.
49. H. Beckers, H. Willner and M. E. Jacox, *ChemPhysChem*, 2009, **10**, 706.
50. H. Beckers, X. Q. Zeng and H. Willner, *Chem. Eur. J.*, 2010, **16**, 1506.
51. M. L. McKee, *J. Am. Chem. Soc.*, 1995, **117**, 1629.
52. O. B. Gadzhiev, S. K. Ignatov, A. G. Razuvaev and A. E. Masunov, *J. Phys. Chem. A.*, 2009, **113**, 9092.
53. O. B. Gadzhiev, S. K. Ignatov, S. Gangopadhyay, A. E. Masunov and A. I. Petrov, *J. Chem. Theory Comput.*, 2011, **7**, 2021.
54. C. Amatore, S. Arbault, D. Bruce, P. de Oliveira, M. Erard and M. Vuillaume, *Chem. Eur. J.*, 2001, **7**, 4171.
55. D. Quinton, S. Griveau and F. Bedioui, *Electrochem. Commun.*, 2010, **12**, 1446-1449.
56. R. H. Crabtree, *Nat. Chem.*, 2009, **1**, 348.
57. G. de Petris, A. Troiani, M. Rosi, G. Angelini and O. Ursini, *Chem. Eur. J.*, 2009, **15**, 4248.
58. N. Dietl, M. Engeser and H. Schwarz, *Angew. Chem.*, 2009, **48**, 4861.
59. D. M. Murphy, L. E. McDyre, E. Carter, A. Stasch and C. Jones, *Magn. Reson. Chem.*, 2011, **49**, 159.
60. W. Kaim, N. S. Hosmane, S. Zalis, J. A. Maguire and W. N. Lipscomb, *Angew. Chem. Int. Ed.*, 2009, **48**, 5082.
61. W. Kaim and N. S. Hosmane, *J. Chem. Sci. (Bangalore, India)*, 2010, **122**, 7.
62. A. E. Ashley, T. J. Herrington, G. G. Wildgoose, H. Zaher, A. L. Thompson, N. H. Rees, T. Kramer and D. O'Hare, *J. Am. Chem. Soc.*, 2011, **133**, 14727.
63. S. A. Cummings, M. Imura, C. J. Harlan, R. J. Kwaan, I. V. Trieu, J. R. Norton, B. M. Bridgewater, F. Jakle, A. Sundararaman and M. Tilset, *Organometallics*, 2006, **25**, 1565.
64. H. Braunschweig, F. Breher, C.-W. Chiu, D. Gamon, D. Nied and K. Radacki, *Angew. Chem. Int. Ed.*, 2010, **49**, 8975.
65. H. Braunschweig, V. Dyakonov, J. O. C. Jimenez-Halla, K. Kraft, I. Krummenacher, K. Radacki, A. Sperlich and J. Wahler, *Angew. Chem. Int. Ed.*, 2012, **51**, 2977.
66. R. Kinjo, B. Donnadiou, M. A. Celik, G. Frenking and G. Bertrand, *Science*, 2011, **333**, 610.
67. J. C. Walton, M. M. Brahmī, L. Fensterbank, E. Lacote, M. Malacria, Q. Chu, S.-H. Ueng, A. Solov'ev and D. P. Curran, *J. Am. Chem. Soc.*, 2010, **132**, 2350.
68. J. C. Walton, M. M. Brahmī, J. Monot, L. Fensterbank, M. Malacria, D. P. Curran and E. Lacote, *J. Am. Chem. Soc.*, 2011, **133**, 10312.

69. N. Kano, A. Furuta, T. Kambe, J. Yoshino, Y. Shibata, T. Kawashima, N. Mizorogi and S. Nagase, *Eur. J. Inorg. Chem.*, 2012, **2012**, 1584.
70. S. M. Mansell, C. J. Adams, G. Bramham, M. F. Haddow, W. Kaim, N. C. Norman, J. E. McGrady, C. A. Russell and S. J. Udeen, *Chem. Commun.*, 2010, **46**, 5070.
71. T. K. Wood, W. E. Piers, B. A. Keay and M. Parvez, *Chem. Commun.*, 2009, 5147.
72. V. J. Richards, A. L. Gower, J. E. Smith, E. S. Davies, D. Lahaye, A. G. Slater nee Phillips, W. Lewis, A. J. Blake, N. R. Champness and D. L. Kays, *Chem. Commun.*, 2012, **48**, 1751.
73. H. M. Tuononen, T. Chivers, A. Armstrong, C. Fedorchuk and R. T. Boéré, *J. Organomet. Chem.*, 2007, **692**, 2705.
74. H. M. Tuononen and A. F. Armstrong, *Dalton Trans.*, 2006, 1885.
75. S. C. Dorman, R. A. O'Brien, A. T. Lewis, E. A. Salter, A. Wierzbicki, P. W. Hixon, R. E. Sykora, A. Mirjafari and J. H. Davis, Jr., *Chem. Commun.*, 2011, **47**, 9072.
76. R. T. Boéré, S. Kacprzak, M. Kessler, C. Knapp, R. Riebau, S. Riedel, T. L. Roemmele, M. Ruhle, H. Scherer and S. Weber, *Angew. Chem. Int. Ed.*, 2011, **50**, 549.
77. T. B. Lee and M. L. McKee, *Inorg. Chem.*, 2012, **51**, 4205.
78. N. Van, I. Tiritiris, R. F. Winter, B. Sarkar, P. Singh, C. Duboc, A. Munoz-Castro, R. Arratia-Perez, W. Kaim and T. Schleid, *Chem. Eur. J.*, 2010, **16**, 11242.
79. H. Tricas, M. Colon, D. Ellis, S. A. Macgregor, D. McKay, G. M. Rosair, A. J. Welch, I. V. Glukhov, F. Rossi, F. Laschi and P. Zanello, *Dalton Trans.*, 2011, **40**, 4200.
80. H. A. Joly, T. Newton and M. Myre, *Phys. Chem. Chem. Phys.*, 2012, **14**, 367.
81. T. W. Myers, N. Kazem, S. Stoll, R. D. Britt, M. Shanmugam and L. A. Berben, *J. Am. Chem. Soc.*, 2011, **133**, 8662.
82. T. W. Myers and L. A. Berben, *J. Am. Chem. Soc.*, 2011, **133**, 11865.
83. T. W. Myers and L. A. Berben, *Inorg. Chem.*, 2012, **51**, 1480.
84. T. T. Tidwell, in *Stable Radicals: Fundamentals and Applied Aspects of Odd-Electron Compounds*, ed. R. G. Hicks, John Wiley & Sons, Ltd, Chichester, 2010, p. 1.
85. J. R. Veciana and I. Ratera, in *Stable Radicals: Fundamentals and Applied Aspects of Odd-Electron Compounds*, ed. R. G. Hicks, John Wiley & Sons, Ltd, Chichester, 2010, p. 33.
86. Y. N. Morita and S. Nishida, in *Stable Radicals: Fundamentals and Applied Aspects of Odd-Electron Compounds*, ed. R. G. Hicks, John Wiley & Sons, Ltd, Chichester, 2010, p. 81.
87. K. Guérin, M. Dubois, A. Houdayer and A. Hamwi, *J. Fluorine Chem.*, 2012, **134**, 11.
88. K. Haubner, K. Luspai, P. Rapta and L. Dunsch, *Phys. Chem. Chem. Phys.*, 2011, **13**, 13403.
89. Y. Morita, S. Suzuki, K. Sato and T. Takui, *Nat. Chem.*, 2011, **3**, 197.
90. N. B. Shustova, D. V. Peryshkov, I. V. Kuvychko, Y.-S. Chen, M. A. Mackey, C. E. Coumbe, D. T. Heaps, B. S. Confait, T. Heine, J. P. Phillips, S. Stevenson, L. Dunsch, A. A. Popov, S. H. Strauss and O. V. Boltalina, *J. Am. Chem. Soc.*, 2011, **133**, 2672.
91. J. C. Konu, T. Chivers, in *Stable Radicals: Fundamentals and Applied Aspects of Odd-Electron Compounds*, ed. R. G. Hicks, John Wiley & Sons, Ltd, Chichester, 2010, p. 317.
92. P. P. Power, *Chem. Rev.*, 2003, **103**, 789.
93. V. Y. Lee and A. Sekiguchi, *Acc. Chem. Res.*, 2007, **40**, 410.
94. V. Y. Lee, M. Nakamoto and A. Sekiguchi, *Chem. Lett.*, 2008, **37**, 128.
95. W. D. Woodul, E. Carter, R. Müller, A. F. Richards, A. Stasch, M. Kaupp, D. M. Murphy, M. Driess and C. Jones, *J. Am. Chem. Soc.*, 2011, **133**, 10074.
96. A. C. Filippou, A. Barandov, G. Schnakenburg, B. Lewall, M. van Gastel and A. Marchanka, *Angew. Chem.*, 2012, **51**, 789.
97. H. Tanaka, M. Ichinohe and A. Sekiguchi, *J. Am. Chem. Soc.*, 2012, **134**, 5540.
98. C. Drost, J. Griebel, R. Kirmse, P. Lönnecke and J. Reinhold, *Angew. Chem. Int. Ed.*, 2009, **48**, 1962.
99. D. Sheberla, B. Tumanskii, D. Bravo-Zhivotovskii, G. Molev, V. Molev, V. Y. Lee, K. Takanashi, A. Sekiguchi and Y. Apeloig, *Organometallics*, 2010, **29**, 5596.

100. M. Becker, C. Foerster, C. Franzen, J. Hartrath, E. Kirsten, J. Knuth, K. W. Klinkhammer, A. Sharma and D. Hinderberger, *Inorg. Chem.*, 2008, **47**, 9965.
101. J. Y. Becker, V. Y. Lee, M. Nakamoto, A. Sekiguchi, A. Chrostowska and A. Dargelos, *Chem. Eur. J.*, 2009, **15**, 8480.
102. A. Chrostowska, A. Dargelos, A. Graciaa, P. Baylere, V. Y. Lee, M. Nakamoto and A. Sekiguchi, *Organometallics*, 2008, **27**, 2915.
103. D. Kurzbach, S. L. Yao, D. Hinderberger and K. W. Klinkhammer, *Dalton Trans.*, 2010, **39**, 6449.
104. D. Kurzbach, A. Sharma, D. Sebastiani, K. W. Klinkhammer and D. Hinderberger, *Chem. Sci.*, 2011, **2**, 473.
105. G. Molev, B. Tumanskii, D. Sheberla, M. Botoshansky, D. Bravo-Zhivotovskii and Y. Apeloig, *J. Am. Chem. Soc.*, 2009, **131**, 11698.
106. T. Nozawa, M. Nagata, M. Ichinohe and A. Sekiguchi, *J. Am. Chem. Soc.*, 2011, **133**, 5773.
107. S. Inoue, M. Ichinohe and A. Sekiguchi, *J. Am. Chem. Soc.*, 2008, **130**, 6078.
108. A. Schafer, M. Weidenbruch, T. Muller, K. Pravinkumar and J. Y. Becker, *Chem. Eur. J.*, 2009, **15**, 8424.
109. B. M. McCollum, J. C. Brodovitch, J. A. Clyburne, A. Mitra, P. W. Percival, A. Tomasik and R. West, *Chem. Eur. J.*, 2009, **15**, 8409.
110. S. Soualmi, L. Ignatovich and V. Jouikov, *Appl. Organomet. Chem.*, 2010, **24**, 865.
111. T. Zoller, C. Dietz, L. Iovkova-Berends, O. Karsten, G. Bradtmoller, A. K. Wiegand, Y. Wang, V. Jouikov and K. Jurkschat, *Inorg. Chem.*, 2012, **51**, 1041.
112. S. Ishida, F. Hirakawa and T. Iwamoto, *J. Am. Chem. Soc.*, 2011, **133**, 12968.
113. R. Edge, R. J. Less, E. J. L. McInnes, K. Muther, V. Naseri, J. M. Rawson and D. S. Wright, *Chem. Commun.*, 2009, 1691.
114. O. Back, M. A. Celik, G. Frenking, M. Melaimi, B. Donnadiu and G. Bertrand, *J. Am. Chem. Soc.*, 2010, **132**, 10262.
115. O. Back, B. Donnadiu, M. von Hopffgarten, S. Klein, R. Tonner, G. Frenking and G. Bertrand, *Chem. Sci.*, 2011, **2**, 858.
116. A. Özbolat-Schön, M. Bode, G. Schnakenburg, A. Anoop, M. van Gastel, F. Neese and R. Streubel, *Angew. Chem. Int. Ed.*, 2010, **49**, 6894.
117. O. Back, B. Donnadiu, P. Parameswaran, G. Frenking and G. Bertrand, *Nat. Chem.*, 2010, **2**, 369.
118. R. Kinjo, B. Donnadiu and G. Bertrand, *Angew. Chem.*, 2010, **49**, 5930.
119. V. Y. Lee, M. Kawai, A. Sekiguchi, H. Ranaivonjatovo and J. Escudié, *Organometallics*, 2009, **28**, 4262.
120. M. Lejeune, P. Grosshans, T. Berclaz, H. Sidorenkova, C. Besnard, P. Pattison and M. Geoffroy, *New. J. Chem.*, 2011, **35**, 2510.
121. M. P. Washington, J. L. Payton, M. C. Simpson and J. D. Protasiewicz, *Organometallics*, 2011, **30**, 1975.
122. C. F. Pi, Y. Wang, W. J. Zheng, L. Wan, H. Y. Wu, L. H. Weng, L. M. Wu, Q. S. Li and P. V. Schleyer, *Angew. Chem. Int. Ed.*, 2010, **49**, 1842.
123. R. T. Boéré, A. M. Bond, S. Cronin, N. W. Duffy, P. Hazendonk, J. D. Masuda, K. Pollard, T. L. Roemmele, P. Tran and Y. Zhang, *New. J. Chem.*, 2008, **32**, 214.
124. S. Sasaki and M. Yoshifuji, *Curr. Org. Chem.*, 2007, **11**, 17.
125. K. Sutoh, S. Sasaki and M. Yoshifuji, *Inorg. Chem.*, 2006, **45**, 992.
126. S. Sasaki, K. Ogawa, M. Watanabe and M. Yoshifuji, *Organometallics*, 2010, **29**, 757.
127. S. Sasaki, M. Murakami, F. Murakami and M. Yoshifuji, *Heteroat. Chem.*, 2011, **22**, 506.
128. R. T. Boéré and M. Taghavikish, *Unpubl. Results*.
129. S. Sasaki, K. Sutoh, F. Murakami and M. Yoshifuji, *J. Am. Chem. Soc.*, 2002, **124**, 14830.
130. S. Mandal, R. Liu, A. C. Reber, M. Qian, H. M. Saavedra, X. Ke, P. Schiffer, S. Sen, P. S. Weiss, S. N. Khanna and A. Sen, *Chem. Commun.*, 2011, **47**, 3126.
131. K. Y. Monakhov, T. Zessin and G. Linti, *Eur. J. Inorg. Chem.*, 2010, 322.
132. I. V. Smolyaninov, A. I. Poddel'skii and N. T. Berberova, *Russ. J. Electrochem.*, 2011, **47**, 1211.
133. N. P. Gritsan, A. Y. Makarov and A. V. Zibarev, *Appl. Magn. Reson.*, 2011, **41**, 449.
134. O. A. Rakitin, *Russ. Chem. Rev.*, 2011, **80**, 647.

135. I. Ratera and J. Veciana, *Chem. Soc. Rev.*, 2012, **41**, 303.
136. R. G. Hicks, in *Stable Radicals: Fundamentals and Applied Aspects of Odd-Electron Compounds*, ed. R. G. Hicks, John Wiley & Sons, Ltd, Chichester, 2010, pp. 317.
137. K. Awaga, in *Encyclopedia of Radicals in Chemistry, Biology and Materials*, John Wiley & Sons, Ltd, Chichester, 2012.
138. T. L. Roemmele, J. Konu, R. T. Boéré and T. Chivers, *Inorg. Chem.*, 2009, **48**, 9454.
139. S. N. Konchenko, N. P. Gritsan, A. V. Lonchakov, U. Radius and A. V. Zibarev, *Mendeleev Commun.*, 2009, **19**, 7.
140. C. L. Kwan, M. Carmack and J. K. Kochi, *J. Phys. Chem.*, 1976, **80**, 1786.
141. N. V. Vasilieva, I. G. Irtegorova, N. P. Gritsan, A. V. Lonchakov, A. Y. Makarov, L. A. Shundrin and A. V. Zibarev, *J. Phys. Org. Chem.*, 2010, **23**, 536.
142. E. A. Suturina, N. A. Semenov, A. V. Lonchakov, I. Y. Bagryanskaya, Y. V. Gatilov, I. G. Irtegorova, N. V. Vasilieva, E. Lork, R. d. Mews, N. P. Gritsan and A. V. Zibarev, *J. Phys. Chem. A*, 2011, **115**, 4851.
143. N. A. Semenov, N. A. Pushkarevsky, A. V. Lonchakov, A. S. Bogomyakov, E. A. Pritchina, E. A. Suturina, N. P. Gritsan, S. N. Konchenko, R. Mews, V. I. Ovcharenko and A. V. Zibarev, *Inorg. Chem.*, 2010, **49**, 7558.
144. E. Lork, R. Mews and A. V. Zibarev, *Mendeleev Commun.*, 2009, **19**, 147.
145. I. S. Morgan, M. Jennings, A. Vindigni, R. Clérac and K. E. Preuss, *Cryst. Growth Des.*, 2011, **11**, 2520.
146. A. Alberola, D. J. Eisler, L. Harvey and J. M. Rawson, *CrystEngComm*, 2011, **13**, 1794.
147. A. Alberola, D. Eisler, R. J. Less, E. Navarro-Moratalla and J. M. Rawson, *Chem. Commun.*, 2010, **46**, 6114.
148. S. V. Potts, L. J. Barbour, D. A. Haynes, J. M. Rawson and G. O. Lloyd, *J. Am. Chem. Soc.*, 2011, **133**, 12948.
149. A. Y. Makarov, V. V. Zhivonitko, A. G. Makarov, S. B. Zikirin, I. Y. Bagryanskaya, V. A. Bagryansky, Y. V. Gatilov, I. G. Irtegorova, M. M. Shakirov and A. V. Zibarev, *Inorg. Chem.*, 2011, **50**, 3017.
150. A. V. Pivtsov, L. V. Kulik, A. Y. Makarov and F. Blockhuys, *Phys. Chem. Chem. Phys.*, 2011, **13**, 3873.
151. A. Decken, A. Mailman, S. M. Mattar and J. Passmore, *Chem. Commun.*, 2005, 2366.
152. A. Decken, A. Mailman and J. Passmore, *Chem. Commun.*, 2009, 6077.
153. A. Decken, A. Mailman, J. Passmore, J. M. Rautiainen, W. Scherer and E. W. Scheidt, *Dalton Trans.*, 2011, **40**, 868.
154. S. M. Mattar and J. Durrelle, *Magn. Reson. Chem.*, 2010, **48 Suppl 1**, S122.
155. W. Fujita, K. Takahashi and H. Kobayashi, *Cryst. Growth Des.*, 2011, **11**, 57.
156. W. Fujita and K. Kikuchi, *Chem. Asian J.*, 2009, **4**, 400.
157. A. A. Leitch, X. Y. Yu, S. M. Winter, R. A. Secco, P. A. Dube and R. T. Oakley, *J. Am. Chem. Soc.*, 2009, **131**, 7112.
158. A. A. Leitch, X. Y. Yu, C. M. Robertson, R. A. Secco, J. S. Tse and R. T. Oakley, *Inorg. Chem.*, 2009, **48**, 9874.
159. S. M. Winter, S. Datta, S. Hill and R. T. Oakley, *J. Am. Chem. Soc.*, 2011, **133**, 8126.
160. J. S. Tse, A. A. Leitch, X. Y. Yu, X. Z. Bao, S. J. Zhang, Q. Q. Liu, C. Q. Jin, R. A. Secco, S. Desgreniers, Y. Ohishi and R. T. Oakley, *J. Am. Chem. Soc.*, 2010, **132**, 4876.
161. A. A. Leitch, K. Lekin, S. M. Winter, L. E. Downie, H. Tsuruda, J. S. Tse, M. Mito, S. Desgreniers, P. A. Dube, S. J. Zhang, Q. Q. Liu, C. Q. Jin, Y. Ohishi and R. T. Oakley, *J. Am. Chem. Soc.*, 2011, **133**, 6051.
162. C. M. Robertson, A. A. Leitch, K. Cvrkalj, R. W. Reed, D. J. T. Myles, P. A. Dube and R. T. Oakley, *J. Am. Chem. Soc.*, 2008, **130**, 8414.
163. C. M. Robertson, A. A. Leitch, K. Cvrkalj, D. J. T. Myles, R. W. Reed, P. A. Dube and R. T. Oakley, *J. Am. Chem. Soc.*, 2008, **130**, 14791.
164. M. Mito, Y. Komorida, H. Tsuruda, J. S. Tse, S. Desgreniers, Y. Ohishi, A. A. Leitch, K. Cvrkalj, C. M. Robertson and R. T. Oakley, *J. Am. Chem. Soc.*, 2009, **131**, 16012.
165. P. A. Yakabuskie, J. M. Joseph, C. R. Stuart and J. C. Wren, *J. Phys. Chem. A*, 2011, **115**, 4270.

166. X. Yu, A. Mailman, K. Lakin, A. Assoud, C. M. Robertson, B. C. Noll, C. F. Campana, J. A. Howard, P. A. Dube and R. T. Oakley, *J. Am. Chem. Soc.*, 2012, **134**, 2264.
167. X. Yu, A. Mailman, K. Lakin, A. Assoud, P. A. Dube and R. T. Oakley, *Cryst. Growth Des.*, 2012, **12**, 2485.
168. S. M. Winter, R. J. Roberts, A. Mailman, K. Cvrkalj, A. Assoud and R. T. Oakley, *Chem. Commun.*, 2010, **46**, 4496.
169. A. Alberola, E. Carter, C. P. Constantinides, D. J. Eisler, D. M. Murphy and J. M. Rawson, *Chem. Commun.*, 2011, **47**, 2532.
170. K. V. Shuvaev, A. Decken, F. Grein, T. S. Abedin, L. K. Thompson and J. Passmore, *Dalton Trans.*, 2008, 4029.
171. M. Deumal, J. M. Rawson, A. E. Goeta, J. A. K. Howard, R. C. B. Copley, M. A. Robb and J. J. Novoa, *Chem. Eur. J.*, 2010, **16**, 2741.
172. C. S. Clarke, D. A. Haynes, J. N. B. Smith, A. S. Batsanov, J. A. K. Howard, S. I. Pascu and J. M. Rawson, *CrystEngComm*, 2010, **12**, 172.
173. C. Allen, D. A. Haynes, C. M. Pask and J. M. Rawson, *CrystEngComm*, 2009, **11**, 2048.
174. D. A. Haynes, *CrystEngComm*, 2011, **13**, 4793.
175. J. M. Rawson, C. S. Clarke and D. W. Bruce, *Mag. Res. Chem.*, 2009, **47**, 3.
176. C. D. Bryan, A. W. Cordes, J. D. Goddard, R. C. Haddon, R. G. Hicks, C. D. MacKinnon, R. C. Mawhinney, R. T. Oakley, T. T. M. Palstra and A. S. Perel, *J. Am. Chem. Soc.*, 1996, **118**, 330.
177. L. G. Hu, A. Iwasaki, R. Suizu, H. Yoshikawa, K. Awaga and H. Ito, *Chem. Phys. Lett.*, 2010, **484**, 177.
178. K. Kanai, H. Yoshida, Y. Noda, A. Iwasaki, R. Suizu, J. y. Tsutumi, H. Imabayashi, Y. Ouchi, N. Sato, K. Seki and K. Awaga, *Phys. Chem. Chem. Phys.*, 2009, **11**, 11432.
179. J. Luzon, J. Campo, F. Palacio, G. J. McIntyre, J. M. Rawson, R. J. Less, C. M. Pask, A. Alberola, R. D. Farley, D. M. Murphy and A. E. Goeta, *Phys. Rev. B.*, 2010, **81**, 144429.
180. R. I. Thomson, E. S. L. Wright, J. M. Rawson, C. J. Howard and M. A. Carpenter, *Phys. Rev. B.*, 2011, **84**, 104450.
181. T. S. Cameron, A. Decken, F. Grein, C. Knapp, J. Passmore, J. M. Rautiainen, K. V. Shuvaev, R. C. Thompson and D. J. Wooll, *Inorg. Chem.*, 2010, **49**, 7861.
182. R. T. Boeré, T. L. Roemmele and X. Yu, *Inorg. Chem.*, 2011, **50**, 5123.
183. K. E. Preuss, *Dalton Trans.*, 2007, 2357.
184. M. T. Lemaire, *Pure Appl. Chem.*, 2011, **83**, 141.
185. M. Kepenekian, B. Le Guennic, K. Awaga and V. Robert, *Phys. Chem. Chem. Phys.*, 2009, **11**, 6066.
186. Y. Umezono, W. Fujita and K. Awaga, *J. Am. Chem. Soc.*, 2006, **128**, 1084.
187. Y. Umezono, W. Fujita and K. Awaga, *Chem. Phys. Lett.*, 2005, **409**, 139.
188. S. S. Staniland, W. Fujita, Y. Umezono, K. Awaga, P. J. Camp, S. J. Clark and N. Robertson, *Inorg. Chem.*, 2005, **44**, 546.
189. K. Awaga, Y. Umezono, W. Fujita, H. Yoshikawa, H. B. Cui, H. Kobayashi, S. S. Staniland and N. Robertson, *Inorg. Chim. Acta.*, 2008, **361**, 3761.
190. N. G. R. Hearn, K. E. Preuss, J. F. Richardson and S. Bin-Salomon, *J. Am. Chem. Soc.*, 2004, **126**, 9942.
191. E. M. Fatila, J. Goodreid, R. Clerac, M. Jennings, J. Assoud and K. E. Preuss, *Chem. Commun.*, 2010, **46**, 6569.
192. N. G. R. Hearn, R. Clérac, M. Jennings and K. E. Preuss, *Dalton Trans.*, 2009, 3193.
193. J. Wu, D. J. MacDonald, R. Clerac, R. Jeon Ie, M. Jennings, A. J. Lough, J. Britten, C. Robertson, P. A. Dube and K. E. Preuss, *Inorg. Chem.*, 2012, **51**, 3827.